Materials and Methods

Isolation of Human Primary T Cells For Gene Targeting

Primary human T cells were isolated from healthy human donors either from fresh whole blood blood samples, residuals from leukoreduction chambers after Trima Apheresis (Blood Centers of the Pacific), or leukapheresis products (StemCell). Peripheral blood mononuclear cells (PBMCs) were isolated from whole blood samples by Ficoll centrifugation using SepMate tubes (STEMCELL, per manufacturer's instructions). T cells were isolated from PBMCs from all cell sources by magnetic negative selection using an EasySep Human T Cell Isolation Kit (STEMCELL, per manufacturer's instructions). Unless otherwise noted, isolated T cells were stimulated and used directly (fresh). When frozen cells were used, previously isolated T cells that had been frozen in Bambanker freezing medium (Bulldog Bio) per manufacturer's instructions were thawed, cultured in media without stimulation for 1 day, and then stimulated and handled as described for freshly isolated samples. Fresh healthy human blood donors were consented under protocol approved by the UCSF Committee on Human Research (CHR). Patient samples for gene editing were obtained under a protocol approved by the Yale Internal Review Board (IRB).

Primary T Cell Culture

Unless otherwise noted, bulk T cells were cultured in XVivo15 medium (STEMCELL) with 5% Fetal Bovine Serum, 50 mM 2-mercaptoethanol, and 10 mM N-Acetyl L-Cystine. Serum free media (ImmunoCult XF T cell expansion media, STEMCELL) without additives, as well as RPMI + 10% FBS were used in indicated experiments (fig. S5). Immediately following isolation, T cells were stimulated for 2 days with anti-human CD3/CD28 magnetic dynabeads (ThermoFisher) at a beads to cells concentration of 1:1, along with a cytokine cocktail of IL-2 at 200 U/mL (UCSF Pharmacy), IL-7 at 5 ng/mL (ThermoFisher), and IL-15 at 5 ng/mL (Life Tech). Following electroporation, T cells were cultured in media with IL-2 at 500 U/mL. Throughout culture T cells were maintained at an approximate density of 1 million cells per mL of media. Every 2-3 days post-electroporation additional media was added, along with additional fresh IL-2 to bring the final concentration to 500 U/mL, and cells were transferred to larger culture vessels as necessary to maintain a density of 1 million cells/mL.

RNP Production

RNPs were produced by annealing of a two-component gRNA to Cas9, as previously described (*7*, *16*). Briefly, crRNAs and tracrRNAs were chemically synthesized (Dharmacon, IDT), and recombinant Cas9-NLS, D10A-NLS, or dCas9-NLS were recombinantly produced and purified (QB3 Macrolab). Lyophilized RNA was resuspended in Tris-HCL (7.4 pH) with 150 mM KCl at a concentration of 160 uM, and stored in aliquots at -80C. crRNA and tracrRNA aliquots were thawed, mixed 1:1 by volume, and incubated at 37C for 30 min to form an 80 uM gRNA solution. Recombinant Cas9 and variants, stored at 40 uM in 20 mM HEPES-KOH pH 7.5, 150 mM KCl, 10% glycerol, 1 mM DTT, were then mixed 1:1 by volume with the 80

uM gRNA (2:1 gRNA to Cas9 molar ratio) at 37C for 15 min to form an RNP at 20 uM. RNPs were generally electroporated immediately after complexing.

dsDNA HDRT Production

Double stranded DNA HDRT sequences were generated from PCR products. Novel HDR sequences were constructed using Gibson Assemblies to place the HDR template sequence, consisting of the homology arms (commonly synthesized as gBlocks from IDT) and the desired insert (such as GFP) into a cloning vector for sequence confirmation and future propagation. These plasmids were used as templates for high-output PCR amplification (Kapa Hotstart polymerase). PCR amplicons (the dsDNA HDRT) were SPRI purified (1.0X) and eluted into a final volume of 3 uL H2O per 100 uL of PCR reaction input. Concentrations of HDRTs were analyzed by nanodrop with a 1:20 dilution. The size of the amplified HDRT was confirmed by gel electrophoresis in a 1.0% agarose gel.

ssDNA HDRT Production by Exonuclease Digestion

To produce long ssDNA as HDR donors, the DNA of interest was amplified via PCR using one regular, non-modified PCR primer and a second phosphorylated PCR primer. The DNA strand that will be amplified using the phosphorylated primer, will be the strand that will be degraded using this method. This allows to either prepare a single stranded sense or single stranded antisense DNA using the respective phosphorylated PCR primer. To produce the ssDNA strand of interest, the phosphorylated strand of the PCR product was degraded via subsequent treatment with two enzymes, Strandase Mix A and Strandase Mix B, for 5 minutes (per 1kb) at 37C, respectively. Enzymes were deactivated by a 5 minute incubation at 80C. Resulting ssDNA HDR templates were SPRI purified (1.0X) and eluted in H2O. A more detailed protocol for the Guide-it™ Long ssDNA Production System (Takara Bio USA, Inc. #632644) can be found at the manufacturer's website.

ssDNA HDRT Production by Reverse Synthesis

ssDNA donors were synthesized by reverse transcription of an RNA intermediate followed by hydrolysis of the RNA strand in the resulting RNA:DNA hybrid product, as described in (*28*). Briefly, the desired HDR donor was first cloned downstream of a T7 promoter and the T7-HDR donor sequence amplified by PCR. RNA was synthesized by in vitro transcription using HiScribe T7 RNA polymerase (New England Biolabs) and reverse-transcribed using TGIRT-III (InGex). Following reverse transcription, NaOH and EDTA were added to 0.2 M and 0.1 M respectively and RNA hydrolysis carried out at 95 ˚C for 10 min. The reaction was quenched with HCl, the final ssDNA product purified using Ampure XP magnetic beads (Beckman Coulter) and eluted in sterile RNAse-free H2O. ssDNA quality was analyzed by capillary electrophoresis (Bioanalyzer, Agilent).

Primary T Cell Electroporations

RNPs and HDR templates were electroporated 2 days following initial T cell stimulation. T cells were harvested from their culture vessels and magnetic CD3/CD28 dynabeads were removed by placing cells on a magnet for 2 minutes. Immediately prior to electroporation, de-beaded cells were centrifuged for 10 minutes at 90g, aspirated, and

resuspended in the Lonza electroporation buffer P3 at 20 uL buffer per one million cells. For optimal editing, one million T cells were electroporated per well using a Lonza 4D 96-well electroporation system with pulse code EH115. Alternate cell concentrations from 200,000 up to 2 million cells per well showed lower efficiencies. Alternate electroporation buffers were used as indicated, but had different optimal pulse settings (EO155 for OMEM buffer). Unless otherwise indicated, 2.5 uLs of RNPs (50 pmols total) were electroporated, along with 2 uLs of HDR Template at 2 ugs/uL (4 ugs HDR Template total).

The order of cell, RNP, and HDRT addition appeared to matter (fig. S1). For 96-well experiments, HDRTs were first aliquoted into wells of a 96-well polypropylene V-bottom plate. RNPs were then added to the HDRTs and allowed to incubate together at RT for at least 30 seconds. Finally, cells resuspended in electroporation buffer were added, briefly mixed by pipetting with the HDRT and RNP, and 24 uLs of total volume (cells + RNP + HDRT) was transferred into a 96 well electroporation cuvette plate. Immediately following electroporation, 80 uLs of pre-warmed media (without cytokines) was added to each well, and cells were allowed to rest for 15 minutes at 37C in a cell culture incubator while remaining in the electroporation cuvettes. After 15 minutes, cells were moved to final culture vessels.

Flow Cytometry

Flow cytometric analysis was performed on an Attune NxT Accustic Focusing Cytometer (ThermoFisher). Surface staining for CD3-APC-eFluor 780 (SK7, eBiosciences), CD4-PerCP (SK3, Tonbo), CD8-PE-Cy7 (SK1, BD), IL2RA/CD25-APC (BC96, Tonbo). Intracellular phosphorylation staining was performed using pStat5(Y694)-PacBlue (clone 47, BD). Intracellular cytokine staining for FoxP3 was performed using FoxP3-AF488 (206D, Biolegend).

Confocal Microscopy

Samples were prepared by drop casting 10 µl of suspended live T cells solution onto a 3x1" microscope slide onto which a 25 mm^2 coverslip was placed. Imaging was performed on an upright configuration Nikon A1r laser scanning confocal microscope. Excitation was achieved through a 488 nm OBIS laser (Coherent). A long working distance (LWD) 60x Plan Apo 1.20 NA water immersion objective was used with additional digital zoom achieved through the NIS-Elements software. Images were acquired under "Galvano" mirror settings with 2x line averaging enabled and exported as TIFF to be analyzed in FIJI (ImageJ, NIH).

CUT&RUN

CUT&RUN was performed on epitope-tagged primary human T cells 11 days after electroporation and 4 days after re-stimulation with anti-CD3/anti-CD28 beads (untagged cells were not electroporated). Approximately 20% and 10% of electroporated cells showed GFP-BATF expression as determined by flow cytometry in donor 1 and donor 2 samples, respectively. CUT&RUN was performed as described in (*18*) using anti-GFP (ab290), anti-BATF (sc-100974), and rabbit anti-mouse (ab46540) antibodies. Briefly, 6 million cells (30 million cells for anti-GFP CUT&RUN in GFP-BATF-containing cells) were collected and washed. Nuclei were isolated and incubated rotating

with primary antibody (GFP or BATF) for 2 hours at 4C. BATF CUT&RUN samples were incubated an additional hour with rabbit anti-mouse antibody. Next, nuclei were incubated with proteinA-micrococcal nuclease (kindly provided by the Henikoff lab) for one hour at 4C. Nuclei were equilibrated to 0C and and MNase digestion was allowed to proceed for 30 minutes. Solubilized chromatin CUT&RUN fragments were isolated and purified. Paired-end sequencing libraries were prepared and run on Illumina Nextseq machines and sequencing data was processed as described in (18). For peak calling and heatmap generation, reads mapping to centromeres were filtered out.

In vitro Treg suppression assay

CD4+ T cells were enriched using the EasySep Human CD4+ T cell enrichment kit (STEMCELL Technologies). CD3+CD4+CD127loCD45RO+TIGIT+ Treg-enriched cells from IL2RA-deficient subjects and HD as well as CD3+CD4+CD25hiCD127lo Tregs from CD25+/- individuals were sorted by flow cytometry. CD3+CD4+CD25-CD127+ responder T cells (Tresps) were labeled with CellTrace CFSE (Invitrogen) at 5 μM. Tregs and HD Tresps were co-cultured at a 1:1 ratio in the presence of beads loaded with anti-CD2, anti-CD3 and anti-CD28 (Treg Suppression Inspector; Miltenyi Biotec) at a 1 bead: 1 cell ratio. On days 3.5 to 4.5, co-cultures were analyzed by FACS for CFSE dilution. % inhibition is calculated using the following formula: 1 – (% proliferation with Tregs / % proliferation of stimulated Tresps without Tregs).

Supplementary Text

Heterozygous/Homozygous integration prediction model

An estimation of the percentage of cells with bi-allelic insertions at a single autosomal genomic locus (two potential alleles) can be made from only fluorescent phenotypes if two HDR templates integrating different fluorescent proteins into that same site are introduced into the cell (electroporated). A simple probability model requires only two assumptions.

> *Assumption 1*: There are no off-target integrations at other sites besides the target locus that contribute to fluorescent phenotypes.
>
> *Assumption 2*: Integration of a specific second fluorescent protein (i.e. RFP) does not depend on which fluorescent protein was integrated at the cell's other allele (i.e. GFP or RFP integrations one the first allele are equally likely to have an RFP integration at the second).

Following the labeling in fig. S13A-C, the percentages of four different phenotypic populations are known:

- % GFP^-RFP^-
- % GFP^+RFP^-
- % GFP^-RFP^+
- % GFP^+RFP^+

From these, immediately two genotypes are known:

1) Genotype A = NA/NA = % GFP^-RFP^-
2) Genotype E = GFP/RFP = % GFP^+RFP^+

The four remaining genotypes sum to the two remaining single fluor positive phenotypes:

3) Genotype B + Genotype D = GFP/NA + GFP/GFP = % GFP^+RFP^-
4) Genotype C + Genotype F = RFP/NA + RFP/RFP = % GFP^-RFP^+

The probabilities that a RFP^+ cell will also be GFP^+, and vice versa, are also known from the phenotypes:

5) Probability of being GFP^+ given being RFP^+ = P(GFP|RFP) = (% GFP^+RFP^+) / (% RFP^+ + %GFP^+RFP^+)
6) Probability of being RFP^+ given being GFP^+ = P(RFP|GFP) = (% GFP^+RFP^+) / (% GFP^+ + %GFP^+RFP^+)

Following from assumption 2, if the probability that a cell receives a GFP integration at its second allele is independent of whether the first integration was a GFP or RFP, then a relationship between the single positive genotypes can be determined (fig S13):

7) $D = P(GFP|RFP) * B$
8) $F = P(RFP|GFP) * C$

Inserting the equations 7 and 8 into equations 3 and 4 respectively and simplifying solves for the remaining genotypes in terms of the known phenotypes:

9) $B = \%\ GFP^{+}RFP^{-} / (1 + (\%\ GFP^{+}RFP^{+}) / (\%\ RFP^{+} + \%GFP^{+}RFP^{+}))$
10) $C = \%\ GFP^{-}RFP^{+} / (1 + (\%\ GFP^{+}RFP^{+}) / (\%\ GFP^{+} + \%GFP^{+}RFP^{+}))$

11) $D = \%\ GFP^{+}RFP^{-} - B$
12) $F = \%\ GFP^{-}RFP^{+} - C$

From the known genotypes, the observed % of cells that are have mono-allelic or bi-allelic insertions, as well as other statistics, can be calculated readily:

- Observed % Cells Heterozygous = B + C
- Observed % Cells Homozygous = D + E + F
- Observed % Cells with at least 1 insertion = B + C + D + E + F = 1 - A = 1 - % GFP-RFP-

- Observed % Alleles that have a GFP = (B + E + 2D) / 2
- Observed % Alleles that have a RNP = (C + E + 2F) / 2
- Observed % Alleles with an insertion = $\%\ Alleles_{GFP} + \%\ Alleles_{RFP}$

An expected % of cells homozygous if the HDR alleles were distributed randomly (in essence at Hardy-Weinberg Equilibrium) can be calculated from the observed % of cells with at least one insertion (HDR):

- p = HDR allele (GFP or RFP)
- q = non-HDR allele (NA)
- X = % of cells observed to have at least one HDR

13) $p + q = 1$
14) $p^2 + 2*p*q + q^2 = 1$

As any cell that has an HDR (GFP or RFP) allele will show the phenotype (in this case GFP+ or RFP+):

15) $X = p^2 + 2*p*q$

Substituting X into equation 14 and simplifying:

16) $q = (1 - X)^{½}$
17) $p = 1 - q$
18) $p = 1 - (1 - X)^{½}$

p^2 will give then give the expected % of cells homozygous for HDR integration if HDR template insertion was random among the target alleles:

19) $p^2 = 2 - 2(1 - X)^{½} - X$

As X is known, the expected % of homozygous cells can be calculated directly from the observed total % of cells with at least one HDR, and can then be compared the observed % of homozygous cells calculated by taking into account the information provided by integration of two separate fluorophores.

Clinical History of Family with Autoimmunity/Immune Dysregulation

The proband is a Caucasian infant who presented at 15 weeks of age after vomiting, fussiness and tachypnea led to medical evaluation that revealed severe diabetic ketoacidosis and serum glucose level of 920 mg/dL. A week after diagnosis, testing for GAD65, IA-2 and insulin autoantibodies was negative; however, autoimmune diabetes was confirmed when repeat antibody tests at 5-7 months of age in three different laboratories showed positive results for IA-2 and insulin autoantibodies, as well as very high levels of GAD65 antibodies in two of the laboratories [42.8 nmol/L (<0.02) at Mayo Laboratories and 896 IU/mL (0.0-5.0) at Barbara Davis Center]. Testing for thyroid dysfunction and celiac disease has been negative but mildly low IgA levels suggest partial IgA deficiency. C-peptide testing was repeatedly completely undetectable, including at 7 months of age when measured 90 minutes after a feed with a serum glucose level of 202 mg/dL, at which time proinsulin was also undetectable. After the initial DKA was treated with intravenous insulin, he was discharged on multiple daily injections of subcutaneous insulin (glargine and lispro) initially and later transitioned to an insulin pump with continuous glucose monitoring. He consistently required a high replacement dose of insulin in the range of 0.8-0.9 units/kg/day (48% basal at 7 months of age). He had been delivered by repeat c-section at 37 weeks gestation with a birth weight of 3.629 kg (75th percentile) without any complications and there have been no concerns about his developmental progress and his medical history has otherwise been unremarkable. His parents have disparate Caucasian ancestry and denied consanguinity.

Clinical information on family members is provided in Table 1. More detailed information is as follows:

1. Mother (37):
    a. Pneumonia as a child – explained as viral
    b. Ear infections as a child treated with antibiotics
    c. Tooth problems (perhaps related to antibiotics)
    d. Her father developed insulin dependent diabetes in his 30's. He had a low WBC and also had nummular dermatitis of the scalp.
    e. Her mother had lupus

2. Father (44)
    a. Moroccan descent

b. No major medical problems
c. Some possible concern this his response time to common viral infections may be prolonged.

3. Affected child (14)
   a. Immune thrombocytopenic purpura: (+ anti-platelet antibodies)
   b. Neutropenia (anti-neutrophil Ab)
   c. Autoimmune hemolytic anemia (DAT+ i.e. direct Coombs+)
   d. Nummular dermatitis of the scalp
   e. Hypercellular bone marrow: inverted CD4/CD8 ratio (0.36).
   f. Mouth ulcers
   g. Ear infections treated with tubes
   h. Diarrhea as a child
   i. 46XX – no known chromosomal abnormality
   j. Flow cytometry of peripheral blood: 82.7% of CD45+ cells are CD3+ and 5.9% are CD19+. CD19+CD5+ cells are the deficient B cells. 43.6% of CD45+ cells are CD8+ with an inverted CD4/CD8 ratio (0.6). There is a relative increase in TCR(alpha beta)+ CD3+ CD4- CD8- T lymphocytes (26% of TCR alpha beta+ CD3+ cells and 5% of CD45+ leukocytes).
   k. Has been treated with immunosuppression including prednisone (20 mg), IgG-pro-IgA, Flonase nasal spray and topical steroids and Symbicort. Also treated with Neupogen.

4. Affected child
   a. 3+ diabetes autoantibodies (anti-GAD, MIAA, ICA, negative ZnT8 and ICA512/IA-2) normal OGTT
   b. Ear infections treated with tubes at 1 yr.
   c. Eczema in the winter

5. Unaffected daughter (15)
   a. Allergies, but otherwise healthy

6. Affected son (4)
   a. Eczema in winter
   b. Positive test for HSV
   c. Insulin dependent diabetes within the first year of life, C-peptide < 0.1 at presentation, anti-GAD ab+ (>30 (nl<1U/ml) 1 yr after dx but negative at dx, ICA512 Ab+ (1.3 (nl<1.0)) 1 yr after dx but negative at dx

7. Unaffected daughter (9)
   a. Asthma

Genetic Testing to Identify *IL2RA* Mutations

Initial genetic testing of the proband using an in-house targeted next-generation sequencing multi-gene panel of over 40 genes known to be involved in monogenic forms of diabetes was negative. Subsequent exome sequencing in the trio pf proband and

parents revealed the causative compound heterozygous mutations in the IL2RA gene. Two siblings carry only one mutation, but the other two with both mutations have evidence for autoimmunity: an older male sibling was found (at 4 or 5 years of age) to have positive diabetes autoantibodies in the absence of hyperglycemia and an older female sibling was diagnosed with autoimmune mediated pancytopenia at age 11 years. CD25 expression was markedly reduced in the three compound heterozygous children.

Clinical Phenotyping of IL2RA Patients

The CD25-deficient children have an almost complete loss of IL2-Ra cell surface expression on T cells and therefore virtually no detectable $CD3^{+}CD4^{+}CD25^{hi}CD127^{lo}$ Tregs in their blood, whereas family relatives carrying heterozygous *IL2RA* mutation display decreased CD25 expression on their Tregs (fig. S20). However, frequencies of $CD3^{+}CD4^{+}CD127^{lo}FOXP3^{+}$ T cells in CD25-deficient subjects resemble those in HD and CD25+/- individuals, thereby suggesting that Tregs may develop in the absence of IL2-Ra function (fig. S20). Using a strategy to isolate Tregs without CD25 expression, we found that $CD3^{+}CD4^{+}CD127^{lo}CD45RO^{+}TIGIT^{+}$ Treg-enriched cells from CD25-deficient subjects showed a defective ability to suppress the proliferation of responder T cells (Tresps) as compared to HD counterparts (fig. S20). In contrast, Tregs from relatives with a single heterozygous *IL2RA* mutation could inhibit Tresp proliferation, although with suboptimum capacity (fig. S20). Hence, correcting functional IL2-Ra expression on the surface of $FOXP3^{+}$ T cells from these patients may represent a valuable approach for developing an *ex vivo* gene therapy.

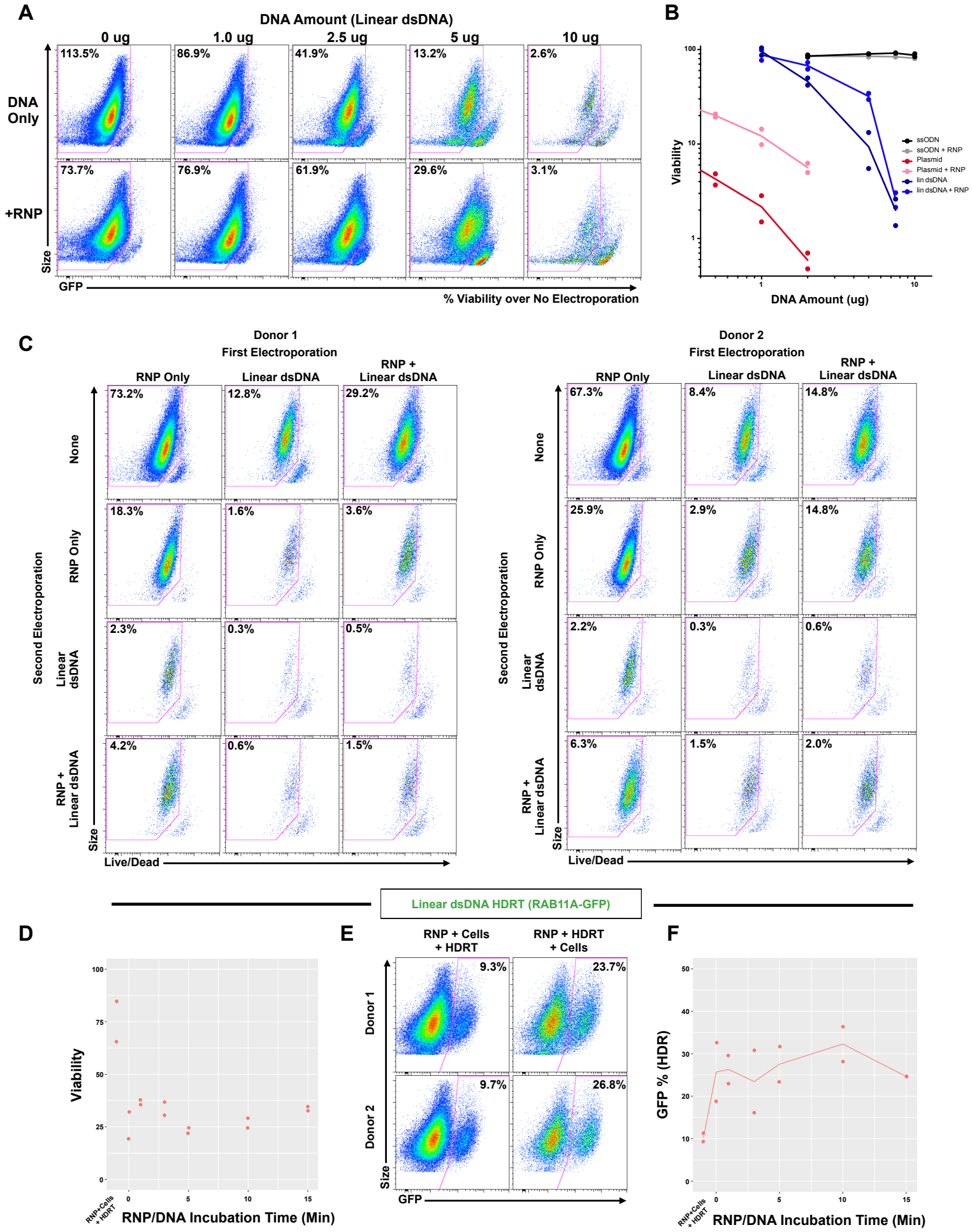
A
DNA Amount (Linear dsDNA)
0 ug
1.0 ug
2.5 ug
5 ug
10 ug
DNA Only
+RNP
113.5%
86.9%
41.9%
13.2%
2.6%
73.7%
76.9%
61.9%
29.6%
3.1%
Size
GFP
% Viability over No Electroporation
B
Viability
DNA Amount (ug)
ssODN
ssODN + RNP
Plasmid
Plasmid + RNP
lin dsDNA
lin dsDNA + RNP
C
Donor 1
First Electroporation
Donor 2
First Electroporation
RNP Only
Linear dsDNA
RNP + Linear dsDNA
Second Electroporation
None
RNP Only
Linear dsDNA
RNP + Linear dsDNA
73.2%
12.8%
29.2%
18.3%
1.6%
3.6%
2.3%
0.3%
0.5%
4.2%
0.6%
1.5%
67.3%
8.4%
14.8%
25.9%
2.9%
14.8%
2.2%
0.3%
0.6%
6.3%
1.5%
2.0%
Size
Live/Dead
Linear dsDNA HDRT (RAB11A-GFP)
D
Viability
RNP/DNA Incubation Time (Min)
RNP+Cells + HDRT
E
RNP + Cells + HDRT
RNP + HDRT + Cells
Donor 1
Donor 2
9.3%
23.7%
9.7%
26.8%
Size
GFP
F
GFP % (HDR)
RNP/DNA Incubation Time (Min)
RNP+Cells + HDRT

Sup Fig 1

Fig. S1. CRISPR/Cas9 RNP co-electroporation reduces dsDNA induced viability loss

(A) A linear dsDNA template (a homology directed repair template, ~1350 bps long, targeting a GFP fusion to *RAB11A*, Fig. 1A) electroporated into primary human T cells cause marked viability loss with increasing amounts of template. Electroporation of the same amount of dsDNA template along with 100 pmols of RNP surprisingly increased viability. **(B)** For both plasmid and linear dsDNA templates, addition of an RNP increased viability post electroporation. Of note, no loss in viability was seen with short ssDNA oligo donor nucleotides (ssODNs). **(C)** RNPs must be delivered concurrently with DNA to see increased viability. T cells from two donors were each electroporated twice with an eight hour rest in between electroporations. While two electroporations so closely interspersed caused a high degree of cell death, delivery of the RNP and linear dsDNA template could be delivered separately. However, an initial RNP electroporation did not increase viability when a DNA template was subsequently electroporated in comparison to cells that received DNA first and RNP second. **(D-F)** Given that the RNP and DNA needed to be introduced concurrently, we assayed whether additional pre-incubation together before electroporation would further increase viability. No difference in viability was seen with increasing pre-incubation time (0 to 15 minutes), but surprisingly if the RNP and cells were mixed first and the DNA template was added immediately prior to elecroporation (RNP + Cells; + HDRT) viability was increased (E). However, in wells where the RNP and the DNA HDR template were mixed together prior to adding the cells (RNP + HDRT; + Cells), no matter how long the RNP and DNA template were preincubated, there was a drastic increase in HDR percentage (GFP+ cells). Viability was measured 2 days following electroporation and GFP expression was measured at day 4. Graphs (B, D, F) display data from 2 healthy human donors.

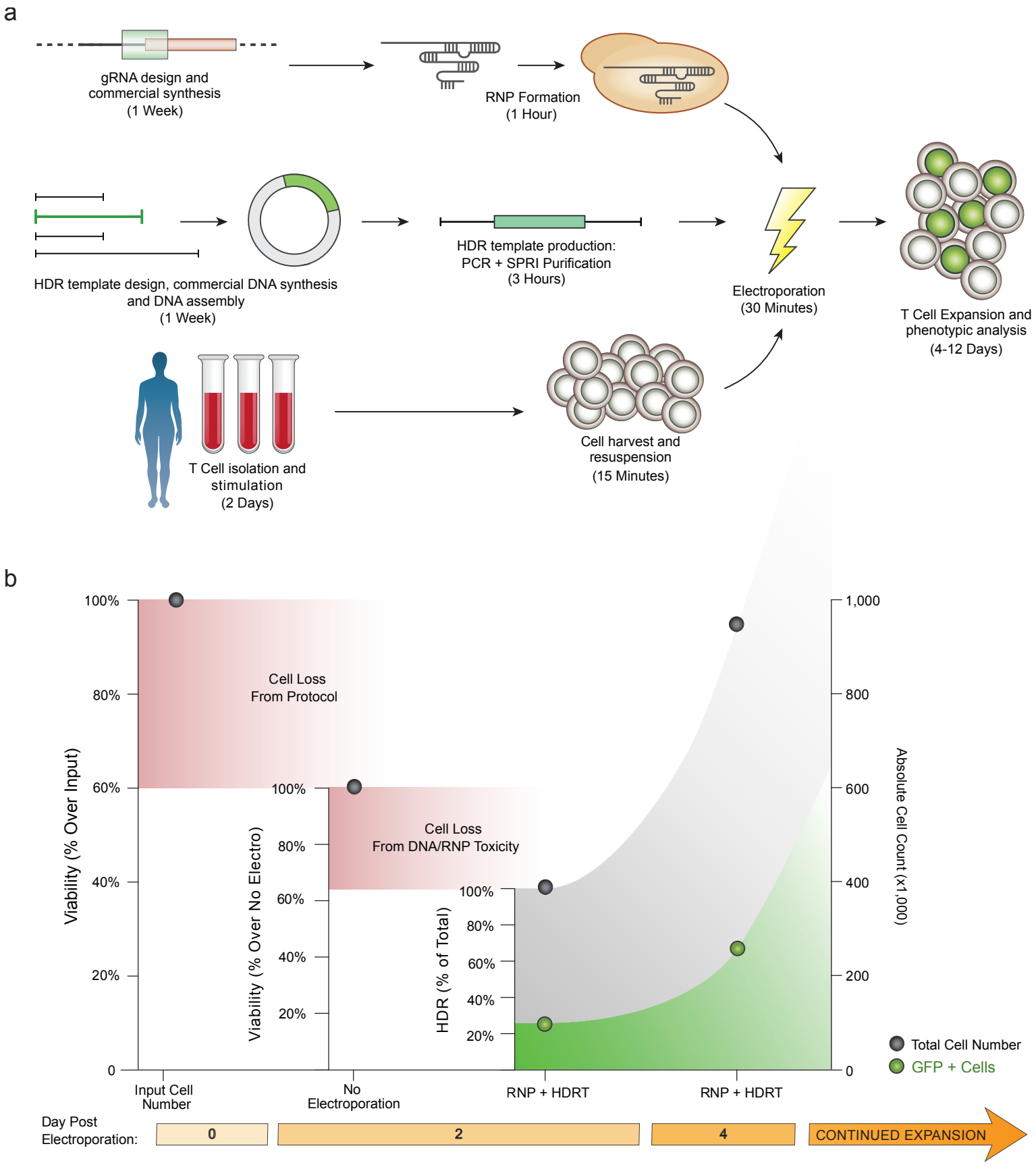
a
gRNA design and commercial synthesis (1 Week)
RNP Formation (1 Hour)
HDR template design, commercial DNA synthesis and DNA assembly (1 Week)
HDR template production: PCR + SPRI Purification (3 Hours)
Electroporation (30 Minutes)
T Cell Expansion and phenotypic analysis (4-12 Days)
T Cell isolation and stimulation (2 Days)
Cell harvest and resuspension (15 Minutes)
b
Viability (% Over Input)
Cell Loss From Protocol
Viability (% Over No Electro)
Cell Loss From DNA/RNP Toxicity
HDR (% of Total)
Absolute Cell Count (x1,000)
Total Cell Number
GFP + Cells
Input Cell Number
No Electroporation
RNP + HDRT
RNP + HDRT
Day Post Electroporation:
0
2
4
CONTINUED EXPANSION

Fig. S2. Non-viral gene targeting enables rapid and efficient genetic engineering in primary human T cells.
(A) Diagrammatic timeline of non-viral gene targeting. Approximately one week is required to design, order from commercial suppliers, and assemble any novel combination of genomic editing reagents (gRNA along with homology directed repair template). Two days prior to electroporation, primary human T cells isolated from blood or various other sources (fig. S5) are stimulated. dsDNA HDR templates can be made easily by PCR followed by a SPRI purification to achieve a highly concentrated product suitable for electroporation. On the day of electroporation, the gRNA complexed to an RNP, the HDR template, and harvested stimulated T cells are mixed and electroporated, a process taking approximately one and a half hours. After electroporation, engineered T cells can be readily expanded for an additional two weeks. **(B)** We use viability to refer to the percentage of live cells relative to an equivalent population that went through all protocol steps except for the actual electroporation (No electroporation control). The trough in live cells after electroporation was empirically determined to come two days following, and all viability measures have been recorded at that time point unless otherwise noted. We use the term efficiency to refer to the percentage of live cells in culture expressing the "knocked in" exogenous sequence (such as GFP). Finally, the total number of cells positive for the desired integration was calculated by multiplying the efficiency by the absolute cell count. Methodological changes that maximized efficiency often were not always optimal for the total number of positive cells, and vice-versa.

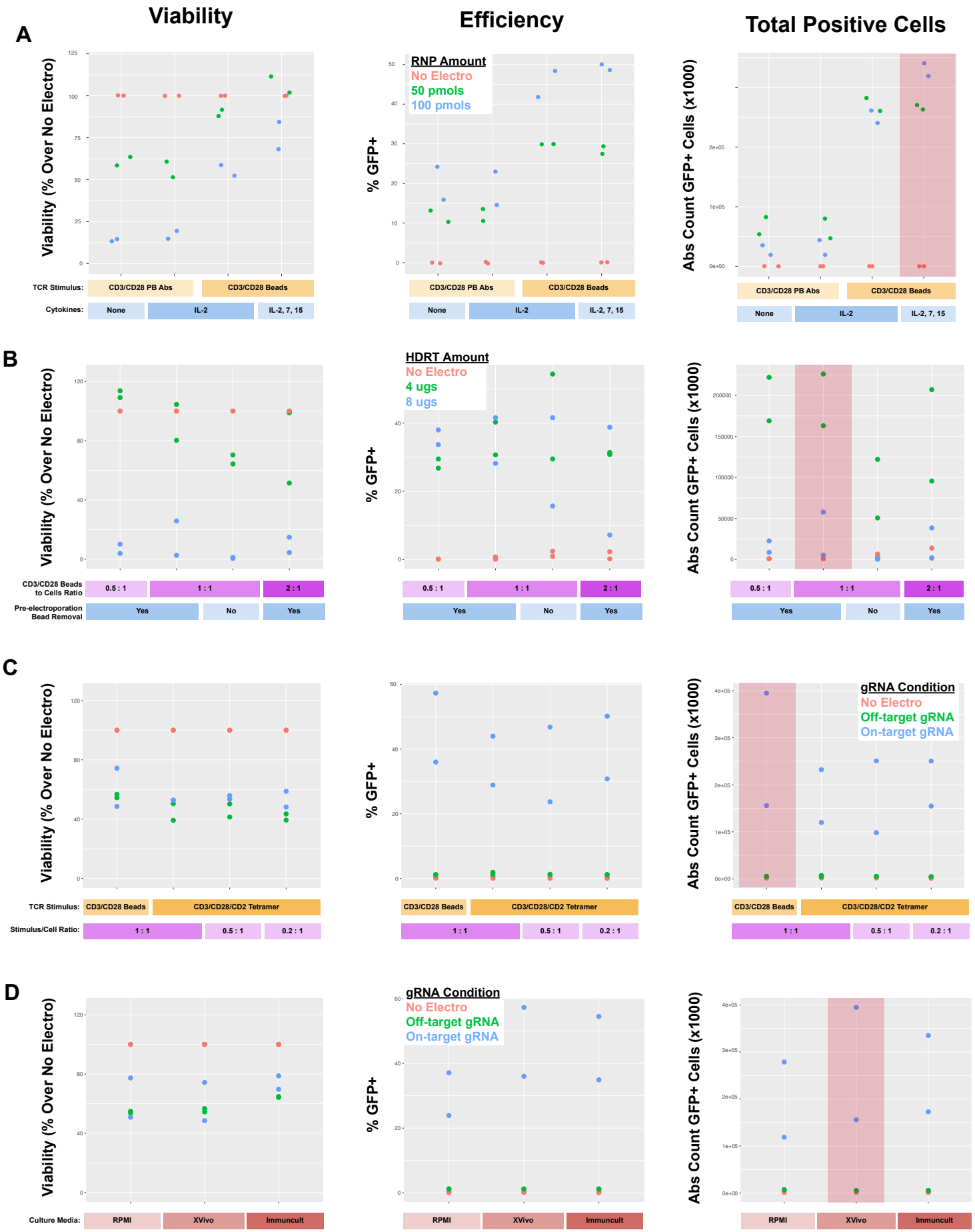
Viability
Efficiency
Total Positive Cells
A
Viability (% Over No Electro)
% GFP+
Abs Count GFP+ Cells (x1000)
RNP Amount
No Electro
50 pmols
100 pmols
TCR Stimulus:
CD3/CD28 PB Abs
CD3/CD28 Beads
Cytokines:
None
IL-2
IL-2, 7, 15
B
HDRT Amount
No Electro
4 ugs
8 ugs
CD3/CD28 Beads to Cells Ratio
0.5 : 1
1 : 1
2 : 1
Pre-electroporation Bead Removal
Yes
No
C
gRNA Condition
No Electro
Off-target gRNA
On-target gRNA
CD3/CD28/CD2 Tetramer
Stimulus/Cell Ratio:
D
Culture Media:
RPMI
XVivo
Immunicult

Sup Fig 3

Fig. S3. Optimization of primary human T cell stimulation for non-viral gene targeting.
(A) Alternative pre-electroporation stimulation conditions were applied for two days prior to electroporation. CD3/CD28 bead bound stimulation along with a cytokine stimulation cocktail of IL-2, IL-7, and IL-15 achieved higher viability, rates of editing, and total positive cells than plate bound antibody stimulation. **(B)** Alternative ratios of beads to cells showed an optimal 1:1 ratio along with removal of beads prior to electroporation. **(C)** Non-bead based CD3/CD28/CD2 stimulation yielded lower editing efficiencies than CD3/CD28 beads at optimal ratio. **(D)** Commercial XVivo15 media achieved similar viability but higher editing efficiencies compared to RPMI. Of interest, the serum-free Immunocult media also enabled high-efficiency editing of human primary CD3+ T cells. Efficiency of GFP insertion (dsDNA RAB11A-GFP HDRT) and the absolute count of total GFP+ cells was performed 4 days following electroporation. Two dots per condition represent the values obtained from two healthy blood donors.

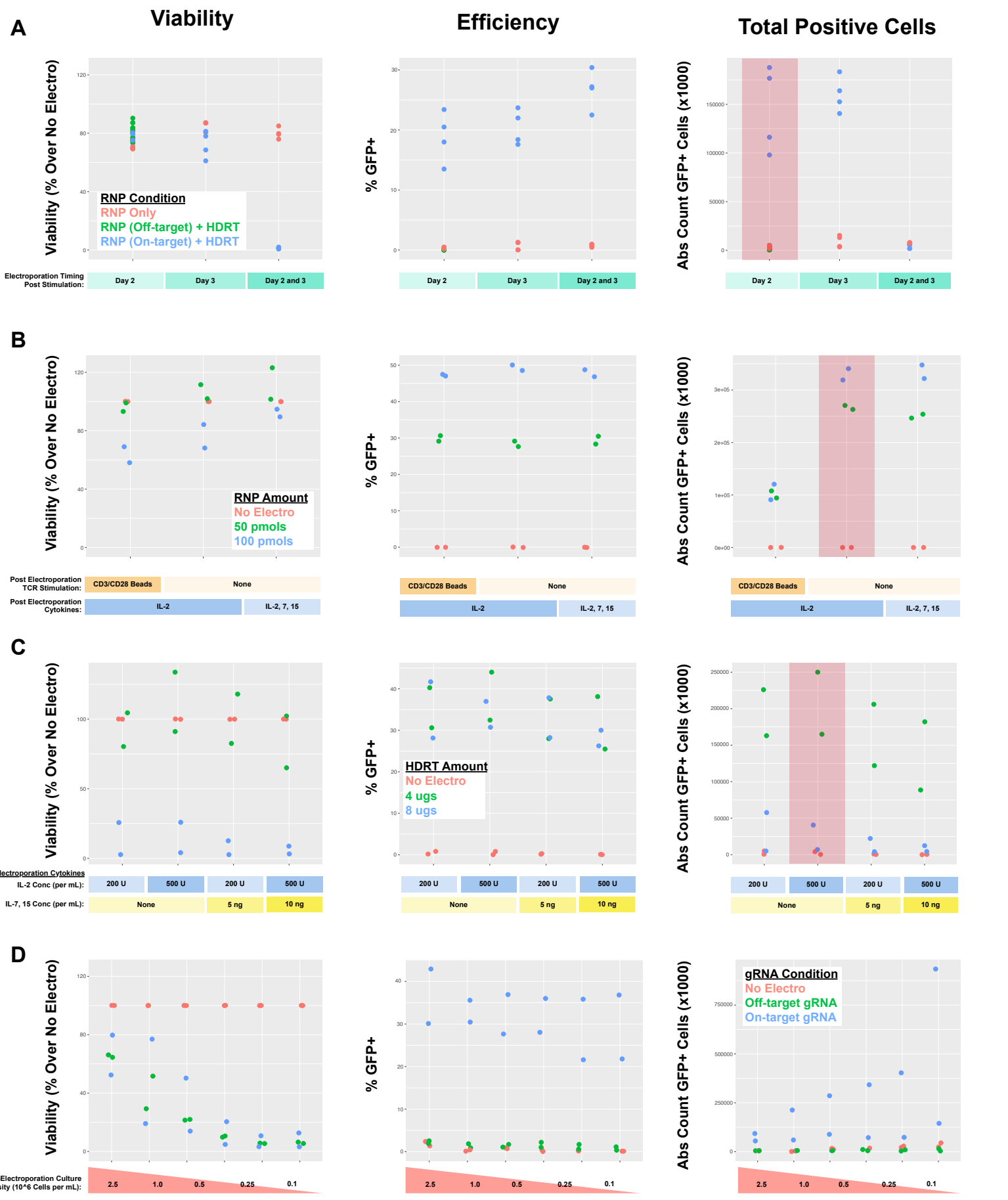
A
Viability
Efficiency
Total Positive Cells
Viability (% Over No Electro)
% GFP+
Abs Count GFP+ Cells (x1000)
RNP Condition
RNP Only
RNP (Off-target) + HDRT
RNP (On-target) + HDRT
Electroporation Timing Post Stimulation:
Day 2
Day 3
Day 2 and 3
B
RNP Amount
No Electro
50 pmols
100 pmols
Post Electroporation TCR Stimulation:
CD3/CD28 Beads
None
Post Electroporation Cytokines:
IL-2
IL-2, 7, 15
C
HDRT Amount
No Electro
4 ugs
8 ugs
Post- Electroporation Cytokines
IL-2 Conc (per mL):
200 U
500 U
IL-7, 15 Conc (per mL):
None
5 ng
10 ng
D
gRNA Condition
No Electro
Off-target gRNA
On-target gRNA
Post-Electroporation Culture Density (10^6 Cells per mL):
2.5
1.0
0.5
0.25
0.1

Sup Fig 4

Fig. S4. Optimization of primary human T cell handling post-electroporation.
(A) Electroporation of CD3+ T cells from healthy human donors at day 2 or day 3 post stimulation achieved efficient targeted GFP integration. Dual electroporations at both days, while increasing efficiency slightly, drastically reduced the viability when a DNA template was included in the two electroporations (fig. S1). **(B)** Additional CD3/CD28 stimulation after electroporation reduced proliferative potential. **(C)** High doses of IL-2 post-electroporation improved both efficiency and viability. Further addition of IL-7 and IL-15, unlike during pre-electroporation stimulation (fig. S3) did not contribute to improved editing. **(D)** Post culture density has little effects on insertion efficiency. Efficiency of GFP insertion (dsDNA RAB11A-GFP HDRT) and the absolute count of total GFP+ cells was performed 4 days following electroporation. Two dots per condition represent the values obtained from two healthy blood donors.

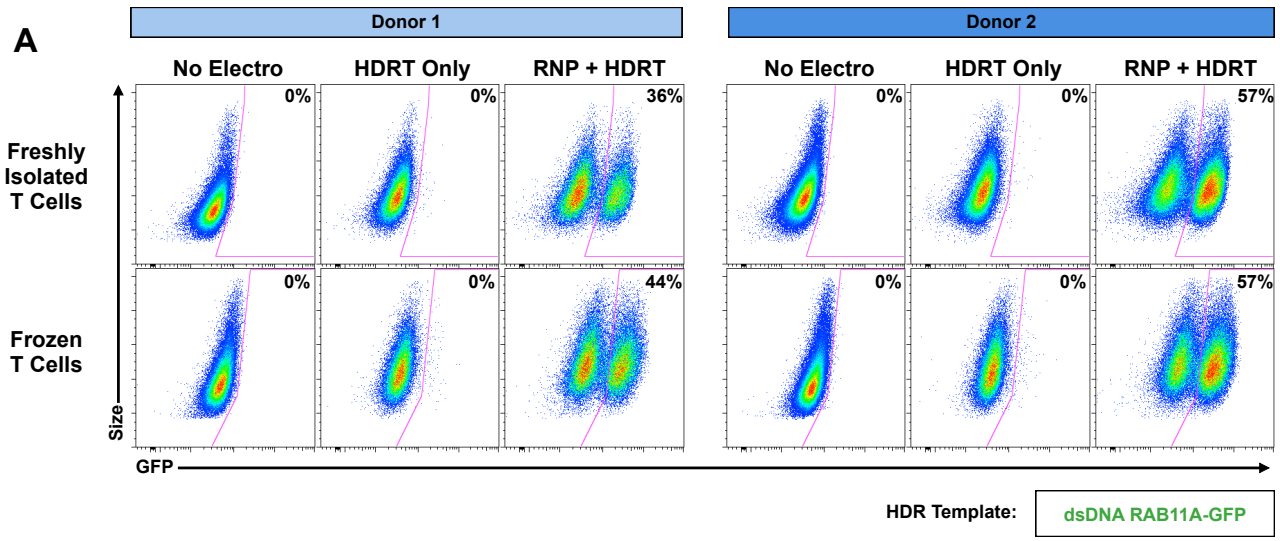
A
Donor 1
Donor 2
No Electro
HDRT Only
RNP + HDRT
No Electro
HDRT Only
RNP + HDRT
Freshly Isolated T Cells
Frozen T Cells
0%
0%
36%
0%
0%
57%
0%
0%
44%
0%
0%
57%
Size
GFP
HDR Template:
dsDNA RAB11A-GFP

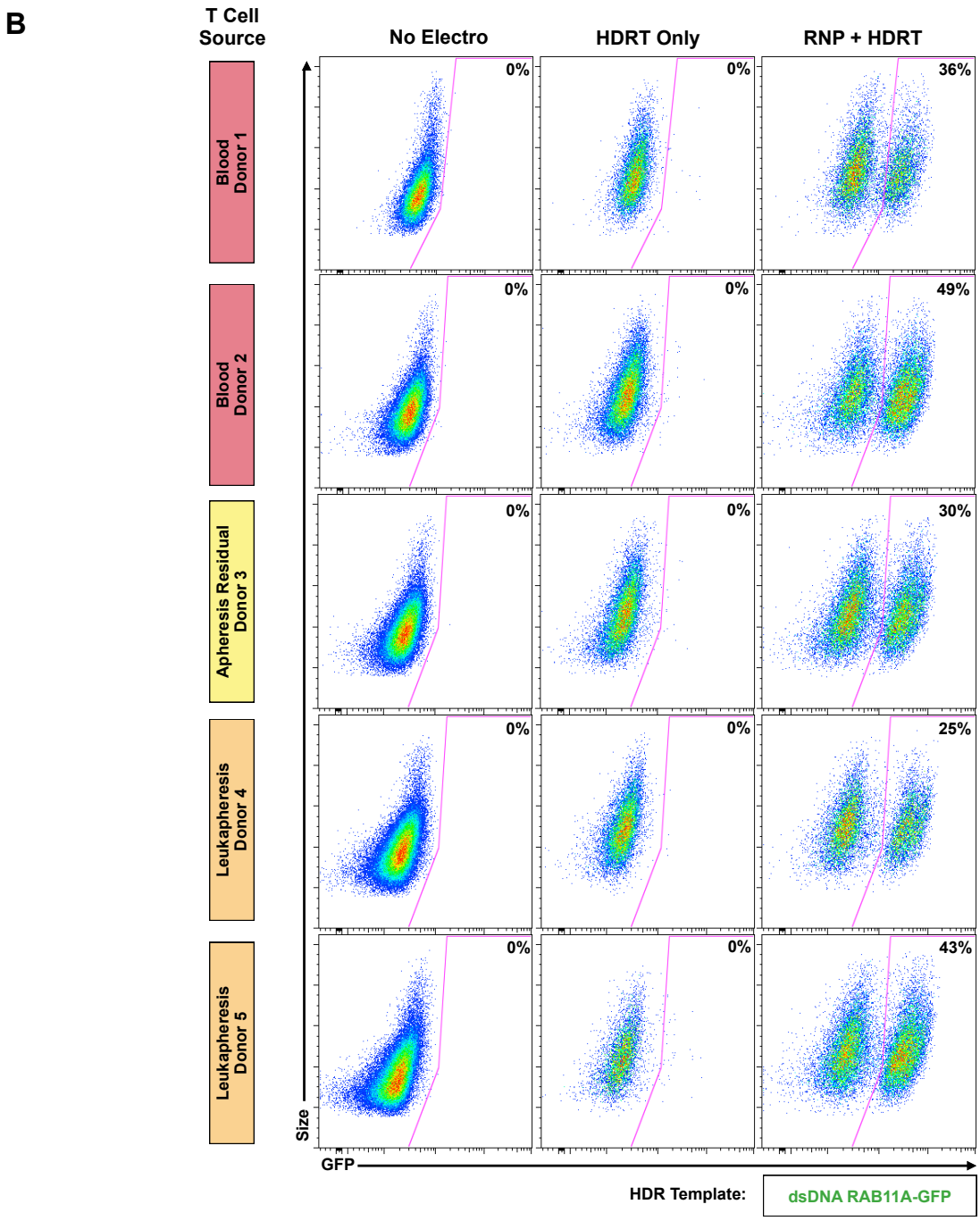
B
T Cell Source
No Electro
HDRT Only
RNP + HDRT
Blood Donor 1
Blood Donor 2
Apheresis Residual Donor 3
Leukapheresis Donor 4
Leukapheresis Donor 5
0%
0%
36%
0%
0%
49%
0%
0%
30%
0%
0%
25%
0%
0%
43%
Size
GFP
HDR Template:
dsDNA RAB11A-GFP

Sup Fig 5

Fig. S5. Efficient non-viral gene targeting in fresh and frozen T cells isolated from multiple sources.
(A) A dsDNA RAB11A-GFP HDR template was inserted into both fresh and frozen T cells from two healthy donors. High rates of GFP insertion were seen in both conditions, demonstrating the adaptability of non-viral gene targeting to research or clinical protocols that require freezing of cells. **(B)** Similarly, high efficiencies of GFP targeted integration were seen in primary human CD3+ T cells isolated from whole blood, a plasma apheresis residual, as well as leukapheresis.

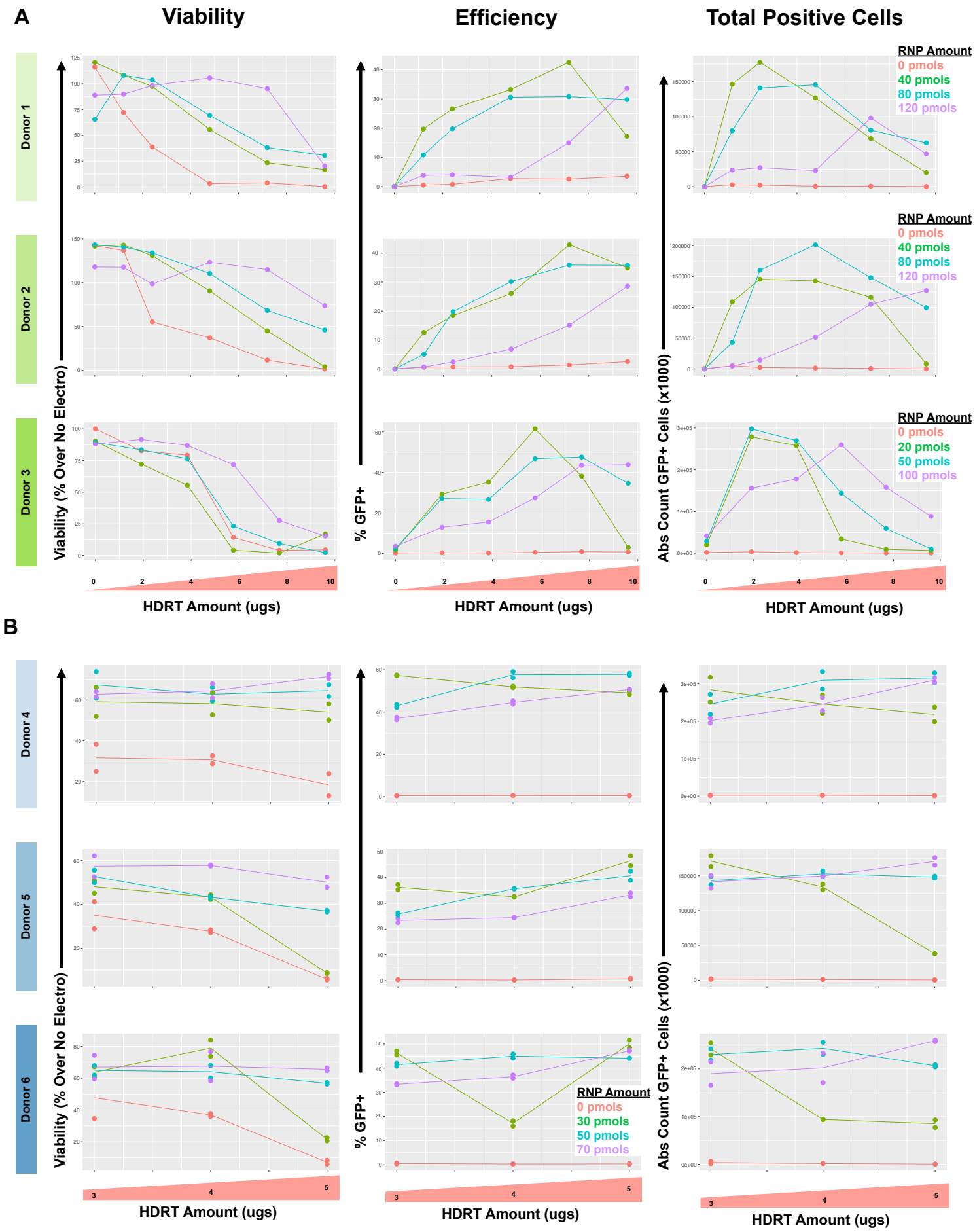
A
Viability
Efficiency
Total Positive Cells
Donor 1
Donor 2
Donor 3
Viability (% Over No Electro)
% GFP+
Abs Count GFP+ Cells (x1000)
RNP Amount
0 pmols
40 pmols
80 pmols
120 pmols
RNP Amount
0 pmols
40 pmols
80 pmols
120 pmols
RNP Amount
0 pmols
20 pmols
50 pmols
100 pmols
HDRT Amount (ugs)
HDRT Amount (ugs)
HDRT Amount (ugs)
B
Donor 4
Donor 5
Donor 6
Viability (% Over No Electro)
% GFP+
Abs Count GFP+ Cells (x1000)
RNP Amount
0 pmols
30 pmols
50 pmols
70 pmols
HDRT Amount (ugs)
HDRT Amount (ugs)
HDRT Amount (ugs)

Sup Fig 6

Fig. S6. Optimization of RNP and HDR template formulations for non-viral gene targeting.
(A) Across three donors, a consistent trend appeared that electroporation of increasing amounts of dsDNA HDR template (RAB11A-GFP) gradually reduced cell viability, while also increasing efficiency, but that intermediate concentrations tested of both HDR template and RNP gave the greatest total number of GFP+ cells. **(B)** Further targeted optimization series in three additional donors yielded an optimal formulation of 4 ugs of HDR template electroporated concurrently with 50 pmols of RNP. Efficiency of GFP insertion and the absolute count of total GFP+ cells was performed 4 days following electroporation. Multiple dots per graph (B) represent technical replicates.

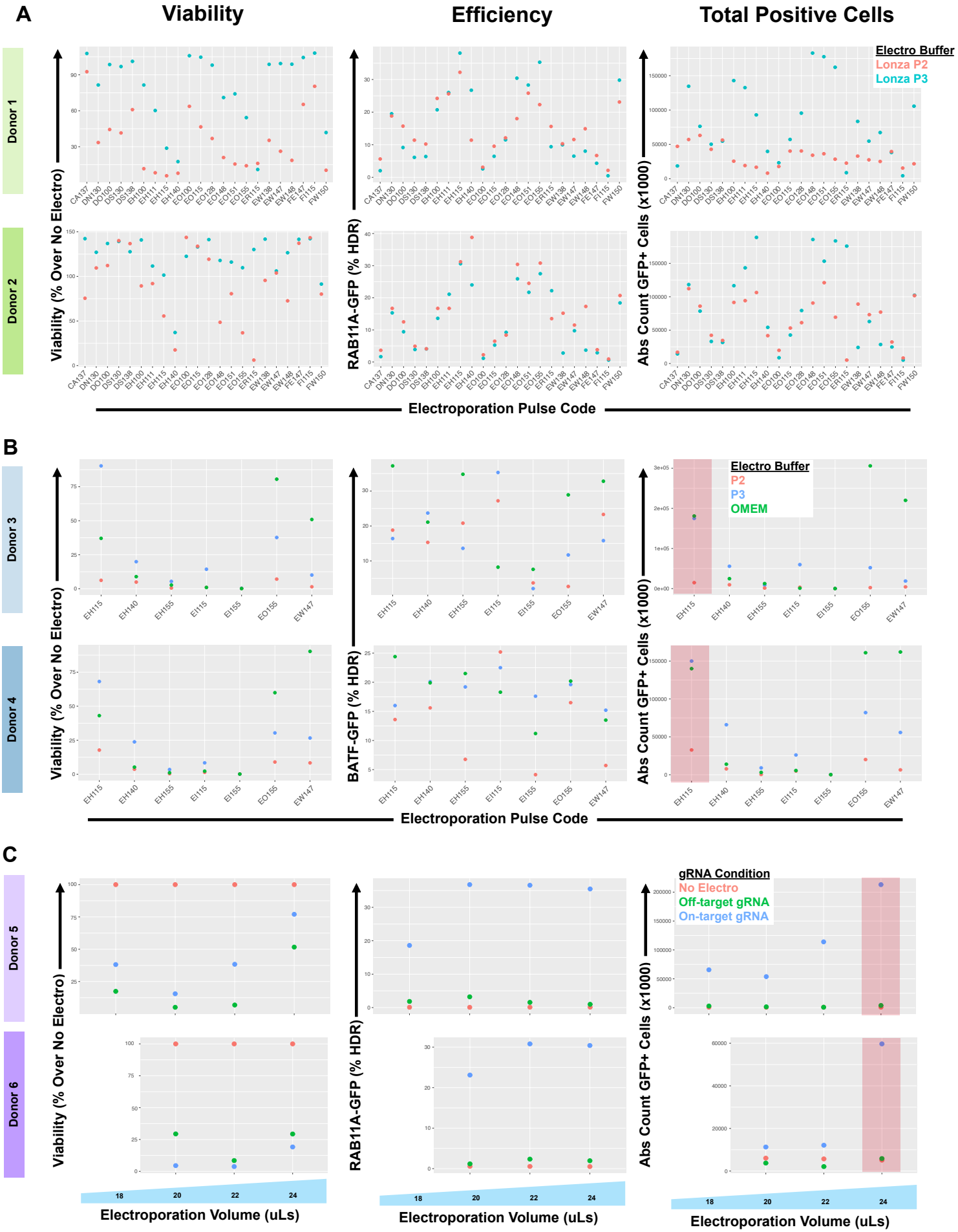
A
Viability
Efficiency
Total Positive Cells
Donor 1
Donor 2
Viability (% Over No Electro)
RAB11A-GFP (% HDR)
Abs Count GFP+ Cells (x1000)
Electro Buffer
Lonza P2
Lonza P3
Electroporation Pulse Code
B
Donor 3
Donor 4
Viability (% Over No Electro)
BATF-GFP (% HDR)
Abs Count GFP+ Cells (x1000)
Electro Buffer
P2
P3
OMEM
Electroporation Pulse Code
C
Donor 5
Donor 6
Viability (% Over No Electro)
RAB11A-GFP (% HDR)
Abs Count GFP+ Cells (x1000)
gRNA Condition
No Electro
Off-target gRNA
On-target gRNA
Electroporation Volume (uLs)
Electroporation Volume (uLs)
Electroporation Volume (uLs)

Sup Fig 7

Fig. S7. Optimization of electroporation parameters for delivery of large non-viral HDR templates.
(A) Raw data shown here is summarized in Fig 1E. Systematic variation of electroporation conditions on a Lonza 4D nucleofector. The ultimately chosen pulse code, EH115, was consistently the most efficient code when using the electroporation buffer Lonza P3. Other alternative codes, such as EO-148 optimized for total positive cells. **(B)** Confirmatory testing of a subset of electroporation conditions also identified pulse code EO-155 in OMEM buffer as a moderate efficiency but high total positive cell combination. **(C)** Electroporating a total volume (RNP + HDRT + Cells) of 24 uL made a large contribution to cell viability and maintained high efficiency. Electroporation volumes above 24 uL commonly cause electroporation failures. Efficiency of dsDNA RAB11A-GFP insertion (A, C) or dsDNA BATF-GFP insertion (B) and the absolute count of total GFP+ cells was performed 4 days following electroporation.

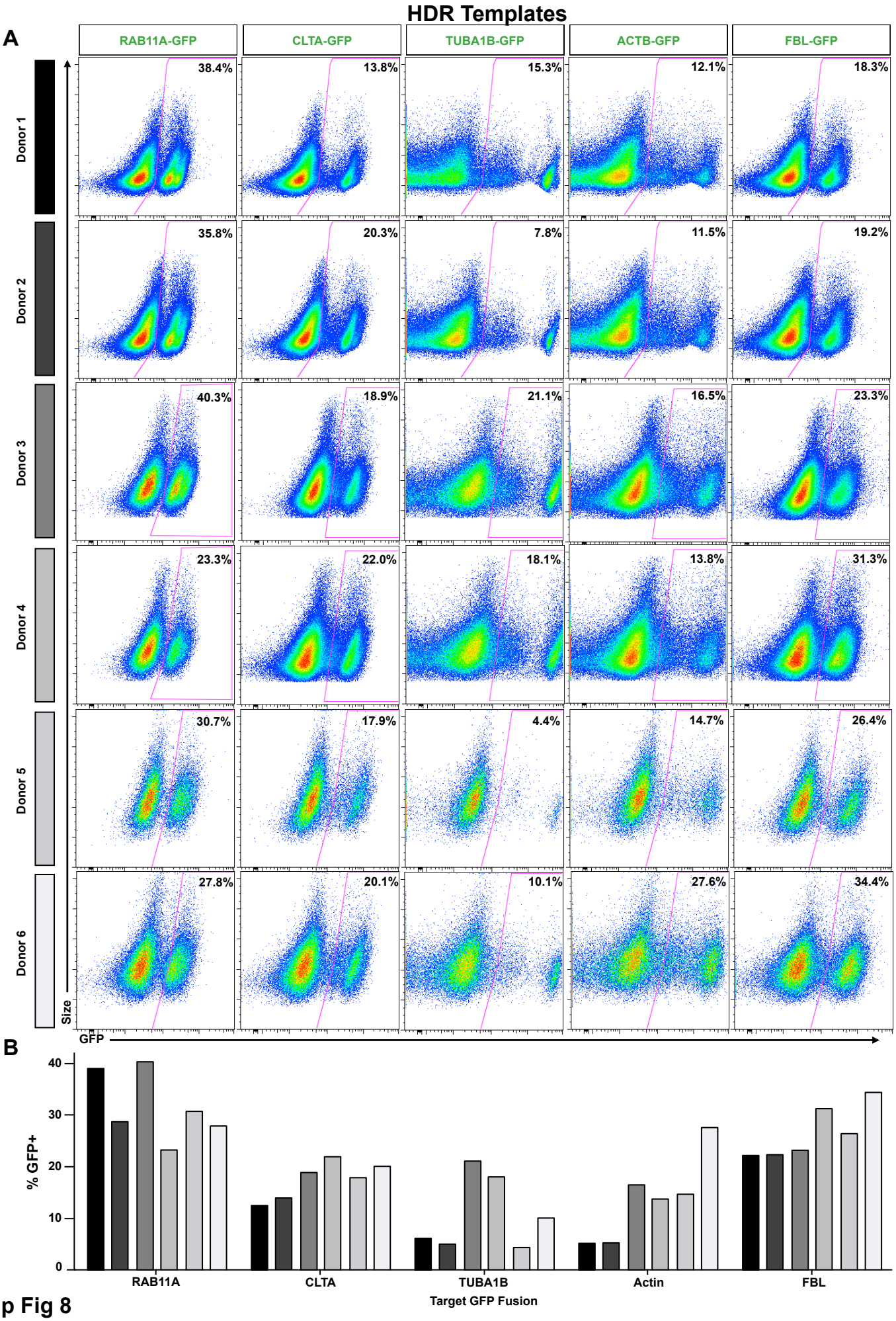
HDR Templates
A
RAB11A-GFP
CLTA-GFP
TUBA1B-GFP
ACTB-GFP
FBL-GFP
Donor 1
Donor 2
Donor 3
Donor 4
Donor 5
Donor 6
38.4%
13.8%
15.3%
12.1%
18.3%
35.8%
20.3%
7.8%
11.5%
19.2%
40.3%
18.9%
21.1%
16.5%
23.3%
23.3%
22.0%
18.1%
13.8%
31.3%
30.7%
17.9%
4.4%
14.7%
26.4%
27.8%
20.1%
10.1%
27.6%
34.4%
Size
GFP
B
% GFP+
40
30
20
10
0
RAB11A
CLTA
TUBA1B
Actin
FBL
Target GFP Fusion

Sup Fig 8

Fig. S8. Reproducible non-viral gene targeting across target loci.
(A) Four days after electroporation of one of five different GFP templates along with a corresponding RNP into primary CD3+CD8+ T cells from six healthy donors, GFP expression is observed across both templates and donors. Note the consistency in GFP expression levels within GFP positive cells across donors for each of the five loci (higher in TUBA1B and ACTB, lower in RAB11A and FBL tags). **(B)** Graphical summary of the percentage of GFP insertion in (A).

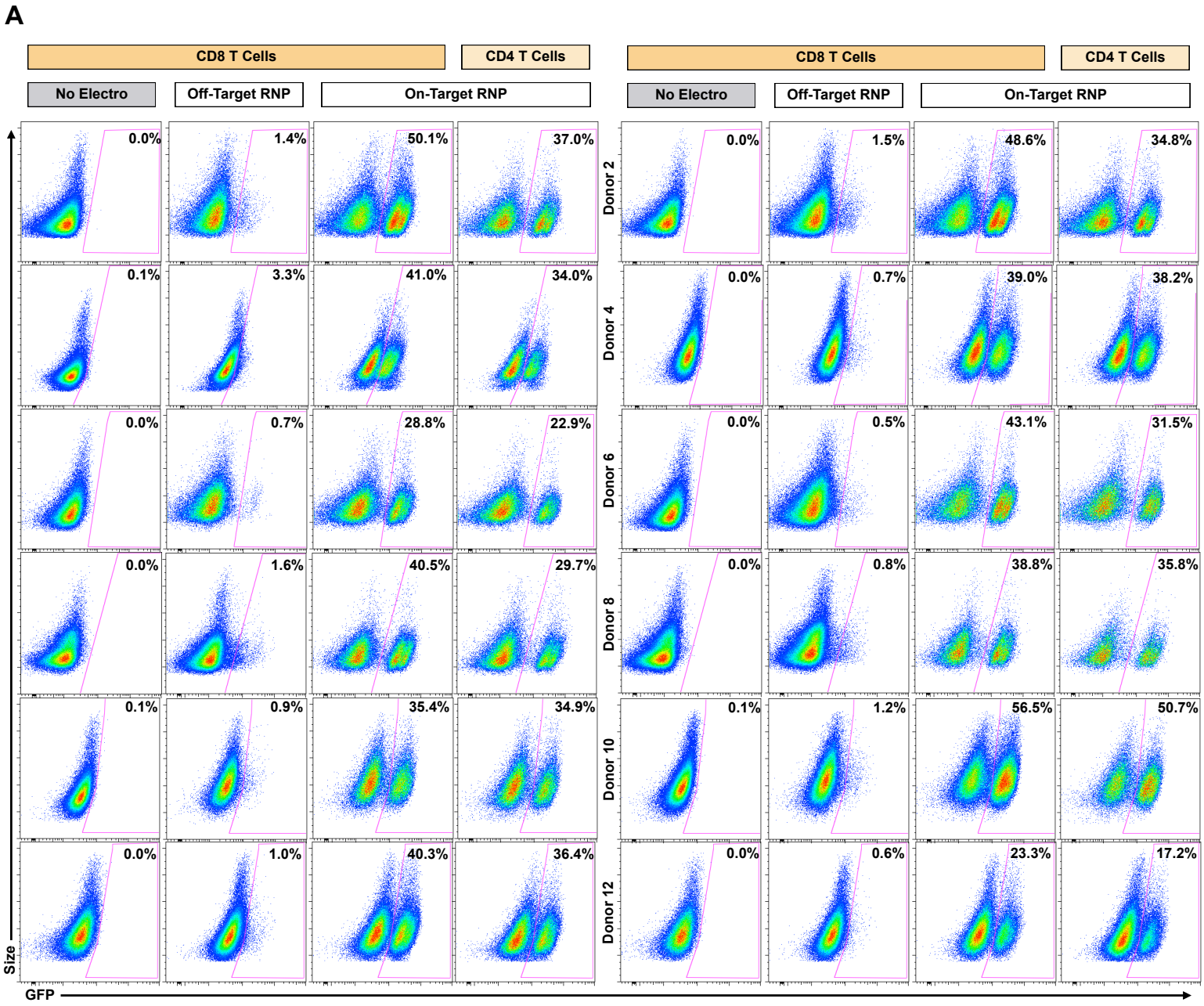

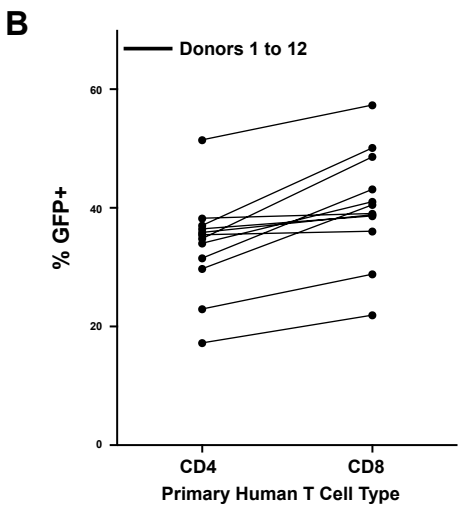

HDR Template: dsDNA RAB11A-GFP

Sup Fig 9

Fig. S9. Reproducible non-viral gene targeting in a cohort of healthy donors.
(A) A constant dsDNA RAB11A-GFP HDR template and RNP was electroporated using the optimized conditions developed for non-viral gene targeting in cells obtained from a cohort of twelve healthy donors. While there was significant variability in GFP insertion percentage among individual donors, all achieved robust integration of GFP (range 22% to 57% in CD8+ T cells). Some GFP expression was seen in cells electroporated with the dsDNA RAB11A-GFP HDR template with an off-target RNP targeting *CXCR4* compared to no-electroporation controls. **(B)** Summary graph of GFP insertion percentages in (**A**). Across the 12 healthy donor cohort slightly higher rates of in GFP expression was seen in CD3+CD8+ T cells (mean 42.0%) compared to CD3+CD4+ T cells (mean 35.2%).

A

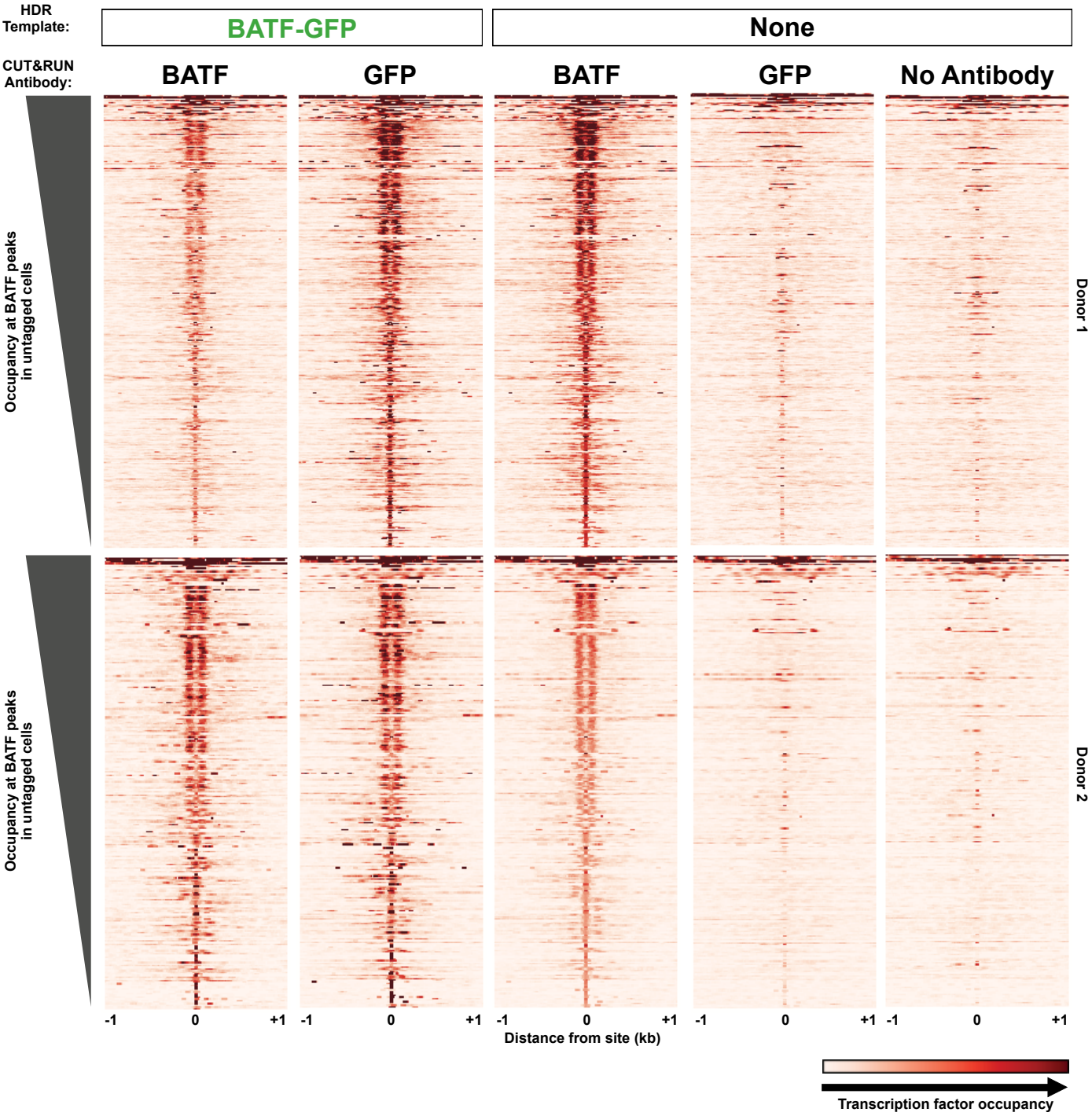
HDR Template:
BATF-GFP
None
CUT&RUN Antibody:
BATF
GFP
BATF
GFP
No Antibody
Occupancy at BATF peaks in untagged cells
Donor 1
Occupancy at BATF peaks in untagged cells
Donor 2
-1
0
+1
Distance from site (kb)
Transcription factor occupancy

Fig. S10. Endogenous tagging of transcription factor BATF for analysis of chromatin occupancy.
Anti-BATF, anti-GFP, and no antibody heatmaps of CUT&RUN data obtained from primary human T cell populations electroporated with GFP-BATF fusion HDR template (untagged cells were not electroporated). Aligned CUT&RUN binding profiles for each sample were centered on BATF CUT&RUN peaks in untagged cells and ordered by BATF peak intensity in untagged cells.

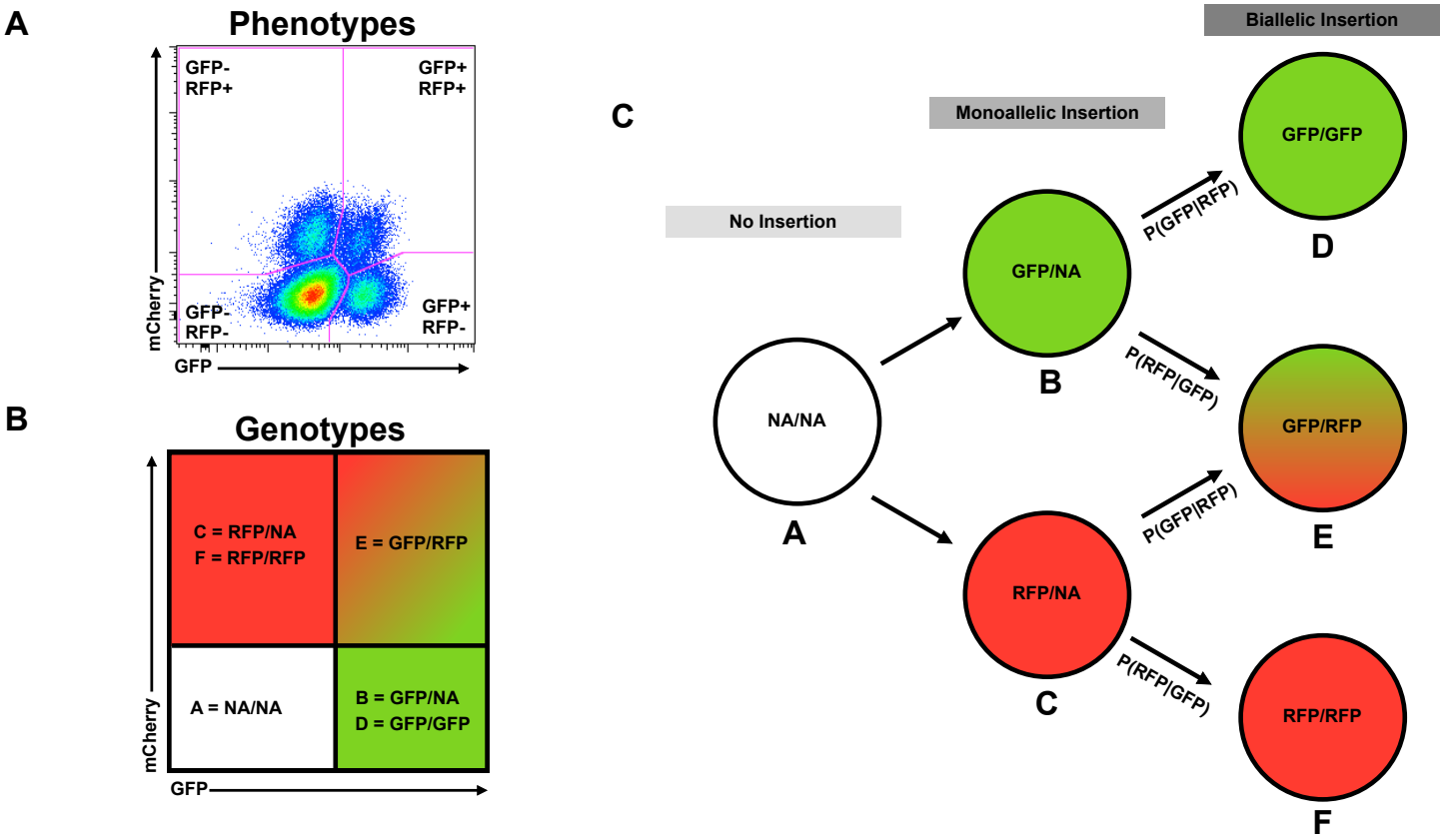
A
Phenotypes
GFP-
RFP+
GFP+
RFP+
GFP-
RFP-
GFP+
RFP-
mCherry
GFP
B
Genotypes
C = RFP/NA
F = RFP/RFP
E = GFP/RFP
A = NA/NA
B = GFP/NA
D = GFP/GFP
mCherry
GFP
C
Biallelic Insertion
Monoallelic Insertion
No Insertion
GFP/GFP
D
GFP/NA
B
NA/NA
A
GFP/RFP
E
RFP/NA
C
RFP/RFP
F
P(GFP|RFP)
P(RFP|GFP)
P(GFP|RFP)
P(RFP|GFP)

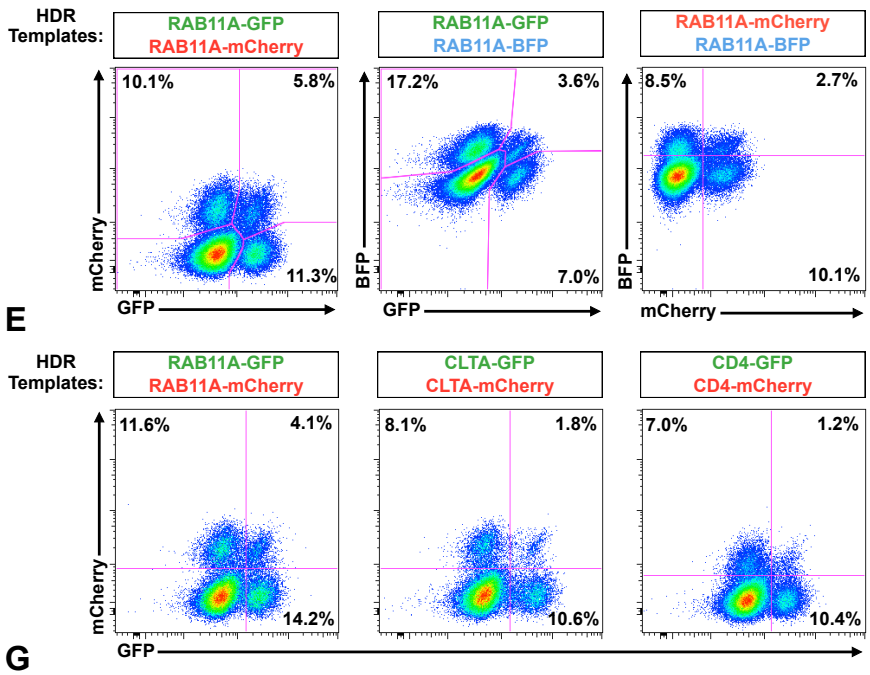
D
HDR Templates:
RAB11A-GFP
RAB11A-mCherry
RAB11A-GFP
RAB11A-BFP
RAB11A-mCherry
RAB11A-BFP
10.1%
5.8%
11.3%
17.2%
3.6%
7.0%
8.5%
2.7%
10.1%
mCherry
GFP
BFP
GFP
BFP
mCherry
E
HDR Templates:
RAB11A-GFP
RAB11A-mCherry
CLTA-GFP
CLTA-mCherry
CD4-GFP
CD4-mCherry
11.6%
4.1%
14.2%
8.1%
1.8%
10.6%
7.0%
1.2%
10.4%
mCherry
GFP

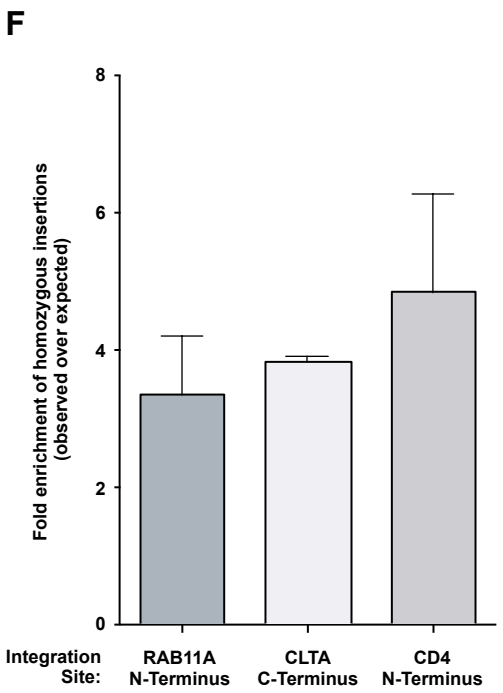
F
Fold enrichment of homozygous insertions
(observed over expected)
0
2
4
6
8
Integration Site:
RAB11A N-Terminus
CLTA C-Terminus
CD4 N-Terminus

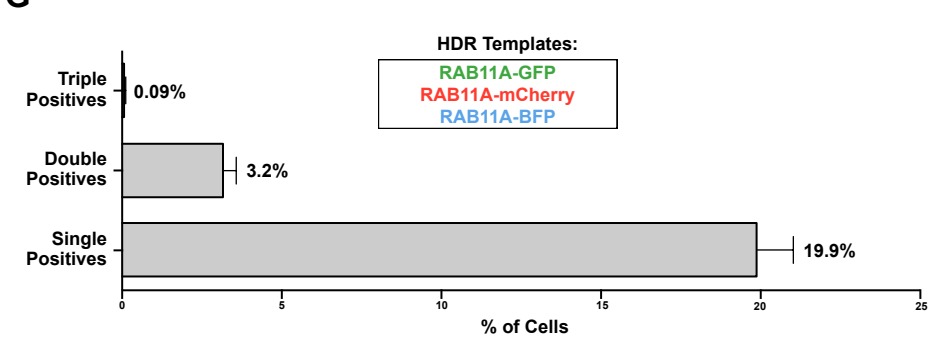
G
HDR Templates:
RAB11A-GFP
RAB11A-mCherry
RAB11A-BFP
Triple Positives
0.09%
Double Positives
3.2%
Single Positives
19.9%
0
5
10
15
20
25
% of Cells

Sup Fig 11

Fig. S11. Modeling and analysis of bi-allelic HDR integrations by insertion of multiple fluorescent proteins into the same locus.
(A) The possible cellular phenotypes when two fluorescent proteins are inserted into the same locus. **(B)** The genotypes of two of these phenotypic populations are immediately known. Cells without any functional insertions (bottom left quadrant, genotype A), must have a NA/NA genotype (where NA indicates an allele without HDR, including WT alleles and NHEJ edited alleles). Dual fluorescent cells (top right quadrant, genotype E) must have acquired one copy of each template (assuming an autosomal target locus and no off-target integrations), and would have a genotype of GFP/RFP. The two single positive populations though will be mixed between cells heterozygous for HDR insertion (Genotypes B and C) or homozygous but for two copies of the same fluorescent template (Genotypes D and F). **(C)** The total percentage of cells with bi-allelic HDR integrations must be the sum of genotypes D, E, and F. While the proportion of cells with genotype E (dual fluor positives) is immediately apparent from the phenotypes, genotypes D and F are not. Application of a simple probability model (supplementary text) allow for the de-convolution of the multiple genotypes in the single fluor positive phenotypes, and thus an estimation of the true percentage of cells homozygous for HDR. **(D)** Bi-allelic HDR analysis applied across a variety of fluorophore permutations inserted into the *RAB11A* locus. **(E-F)** Dual fluorescence bi-allelic integrations were seen across target loci. While the total percentage of cells with an insertion varied with the efficiency of each target site, the fold enrichment in the observed percentage of homozygous cells over that predicted by random chance was consistent across loci. **(G)** Attempted integration of three distinct fluorophores by HDR into the same locus. As a max of two targeted insertions are possible (at the locus' two alleles; assuming a diploid genome), no cells positive for all three loci should be observed (triple positives). Indeed, while large numbers of single fluorophore integrations are observed (single positives), as well as cells positive for the various permutations of two fluors (double positives), there is a 30 fold reduction in the number of triple positive cells compared to double positives. All flow cytometric analysis of fluorescent protein expression was performed 4 days following electroporation. Displays are representative of multiple technical replicates from one (E, F) or two (D, G) healthy human donors. Bar graphs display mean + standard deviation.

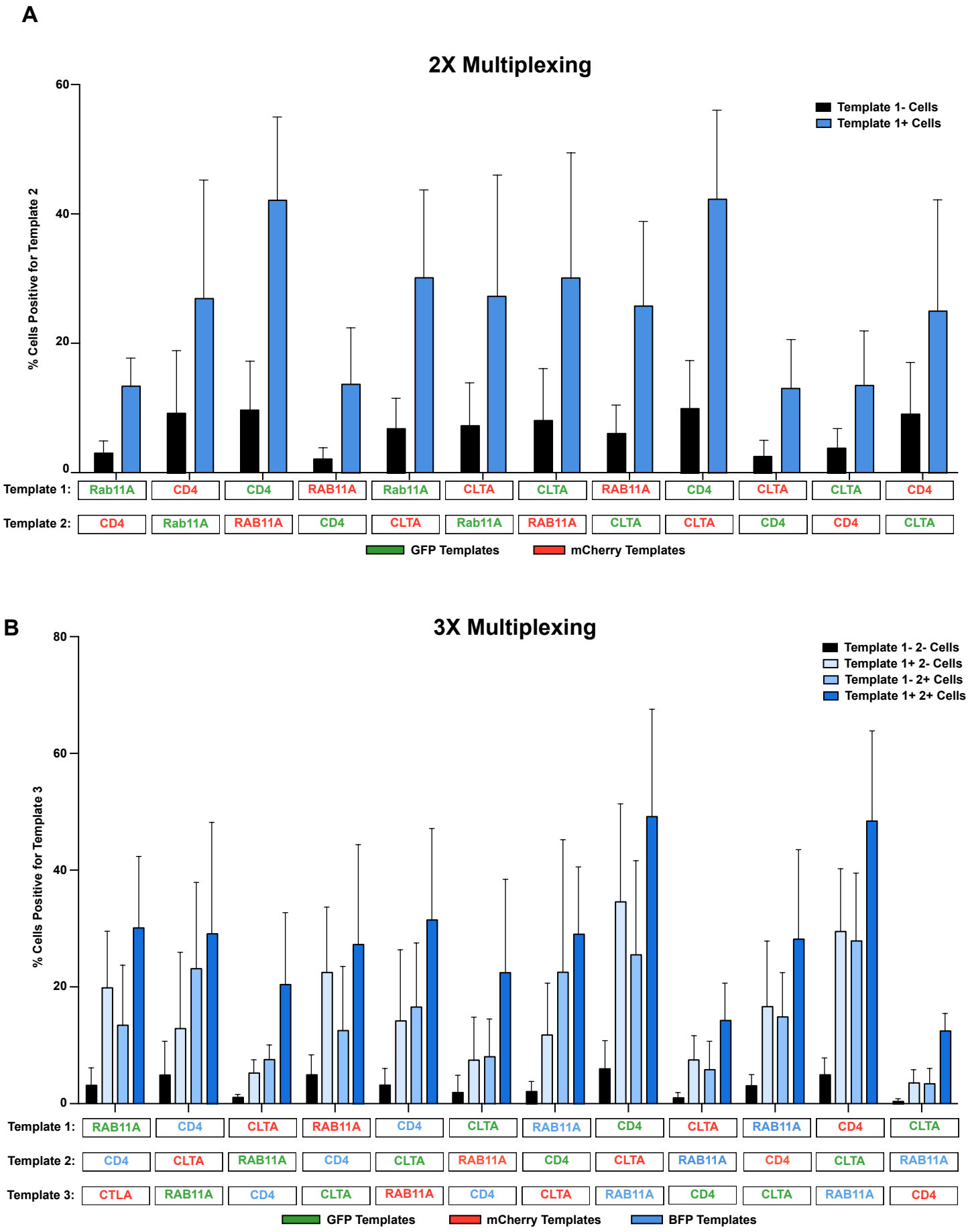
A
2X Multiplexing
% Cells Positive for Template 2
60
40
20
0
Template 1- Cells
Template 1+ Cells
Template 1: Rab11A CD4 CD4 RAB11A Rab11A CLTA CLTA RAB11A CD4 CLTA CLTA CD4
Template 2: CD4 Rab11A RAB11A CD4 CLTA Rab11A RAB11A CLTA CLTA CD4 CD4 CLTA
GFP Templates
mCherry Templates
B
3X Multiplexing
% Cells Positive for Template 3
80
60
40
20
0
Template 1- 2- Cells
Template 1+ 2- Cells
Template 1- 2+ Cells
Template 1+ 2+ Cells
Template 1: RAB11A CD4 CLTA RAB11A CD4 CLTA RAB11A CD4 CLTA RAB11A CD4 CLTA
Template 2: CD4 CLTA RAB11A CD4 CLTA RAB11A CD4 CLTA RAB11A CD4 CLTA RAB11A
Template 3: CTLA RAB11A CD4 CLTA RAB11A CD4 CLTA RAB11A CD4 CLTA RAB11A CD4
GFP Templates
mCherry Templates
BFP Templates

Sup Fig 12

Fig. S12. Multiplexed integrations show that acquisition of HDR integration at one locus increases likelihood of HDR at additional loci.
(A) Two HDR template permutations from a set of six dsDNA HDR templates (targeting RAB11A, CD4, and CLTA; each site with GFP or RFP) were electroporated into CD3+ T cells isolated from healthy human donors. Four days after electroporation of the indicated two HDR templates along with their two respective on-target RNPs, the percentage of cells positive for each template was analyzed when gating on cells either positive or negative for the other template. Not only was two-template multiplexing possible across a variety of template combinations, but gating on cells positive for one template (Template 1+ Cells, Blue) yielded an enriched population of cells more likely to be positive for the second template compared to cells negative for the first (Template 1- Cells, Black). 2 ugs of each template, along with 30 pmols of each associated RNP, were electroporated for dual multiplexing experiments. **(B)** Electroporation of an additional template allows for 3 site multiplexing using a variety of HDR template combinations. Cells positive for the third template can be further enriched by gating on cells positive for both other templates when compared to single positive cells. Displayed data are means + standard deviation from multiple technical replicates from two healthy human donors.

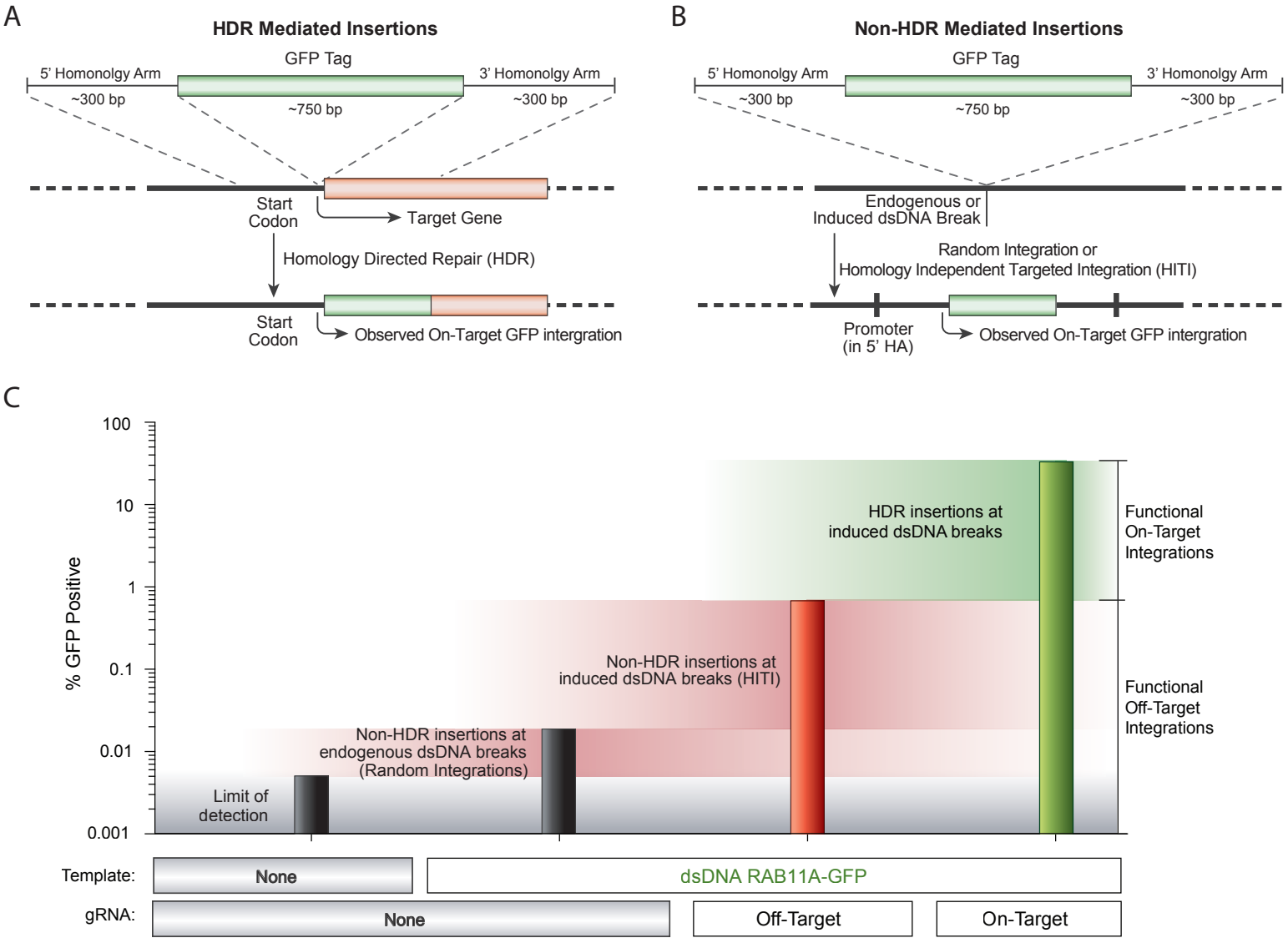
A
HDR Mediated Insertions
5' Homonolgy Arm
~300 bp
GFP Tag
~750 bp
3' Homonolgy Arm
~300 bp
Start Codon
Target Gene
Homology Directed Repair (HDR)
Start Codon
Observed On-Target GFP intergration
B
Non-HDR Mediated Insertions
5' Homonolgy Arm
~300 bp
GFP Tag
~750 bp
3' Homonolgy Arm
~300 bp
Endogenous or Induced dsDNA Break
Random Integration or Homology Independent Targeted Integration (HITI)
Promoter (in 5' HA)
Observed On-Target GFP intergration
C
% GFP Positive
100
10
1
0.1
0.01
0.001
HDR insertions at induced dsDNA breaks
Non-HDR insertions at induced dsDNA breaks (HITI)
Non-HDR insertions at endogenous dsDNA breaks (Random Integrations)
Limit of detection
Functional On-Target Integrations
Functional Off-Target Integrations
Template:
None
dsDNA RAB11A-GFP
gRNA:
None
Off-Target
On-Target
D
% GFP Positive
100
10
1
0.1
0.01
On-Target gRNA
Off-Target gRNA
dsDNA Only
HDR Template:
RAB11A-GFP
CLTA-GFP
TUBA1B-GFP
ACTB-GFP
FBL-GFP

Fig. S13. Fluorescent estimation and quantification of off-target integration events across multiple HDR templates.
(A) Diagram of HDR mediated insertions at the N-terminus of a target locus (not drawn to scale). The homology arms specify the exact sequence where the insert (a GFP tag in this case) will be inserted, allowing for scarless integration of exogenous sequences. As a GFP fusion protein is created, GFP fluorescence will be seen as a result of this on-target integration, dependent on an RNP cutting adjacent to the integration site. **(B)** Double stranded DNA can be integrated via homology-independent repair mechanisms at off-target sites through either random integration at naturally occurring dsDNA breaks, or potentially at induced double stranded breaks, such as those at the off-target cut sites of the RNP. This effect can be harnessed to allow for targeted integration of a dsDNA sequence at a desired induced dsDNA break (HITI) in senescent cell types lacking the ability to do HDR, but crucially the entirety of the dsDNA template is integrated, including any potential homology arms. In the case that the homology arms contain a promoter sequence (such as for N-terminal fusion tags), these off target integrations can drive observable expression of the inserted sequence without the desired correct HDR insertion. **(C)** Bars represent real GFP+ percentages from human CD3+ T cells electorporated with the indicated components. Flow cytometry for fluorescent protein expression can be used to rapidly evaluate functional off-target integrations. The increase in the percentage of fluorescent cells over the limit of detection when the template alone is electroporated likely represents random integrations at naturally occurring dsDNA breaks. Not every off-target integration will yield fluorescent protein expression, but the relative differences in functional off-target expression between different templates can be assayed. Inclusion of an RNP targeting *CXCR4* dramatically increases the observed off-target homology-independent integrations, likely through a HITI-type insertion event. The largest increase (from 1% to >30% in this donor) comes though through electroporation of the correct RNP and HDR mediated insertion. **(D)** Comparisons of on-target GFP expression vs functional off-target integrations across five templates. Mean expression (bars) of two biologic donors (dots) are graphed.

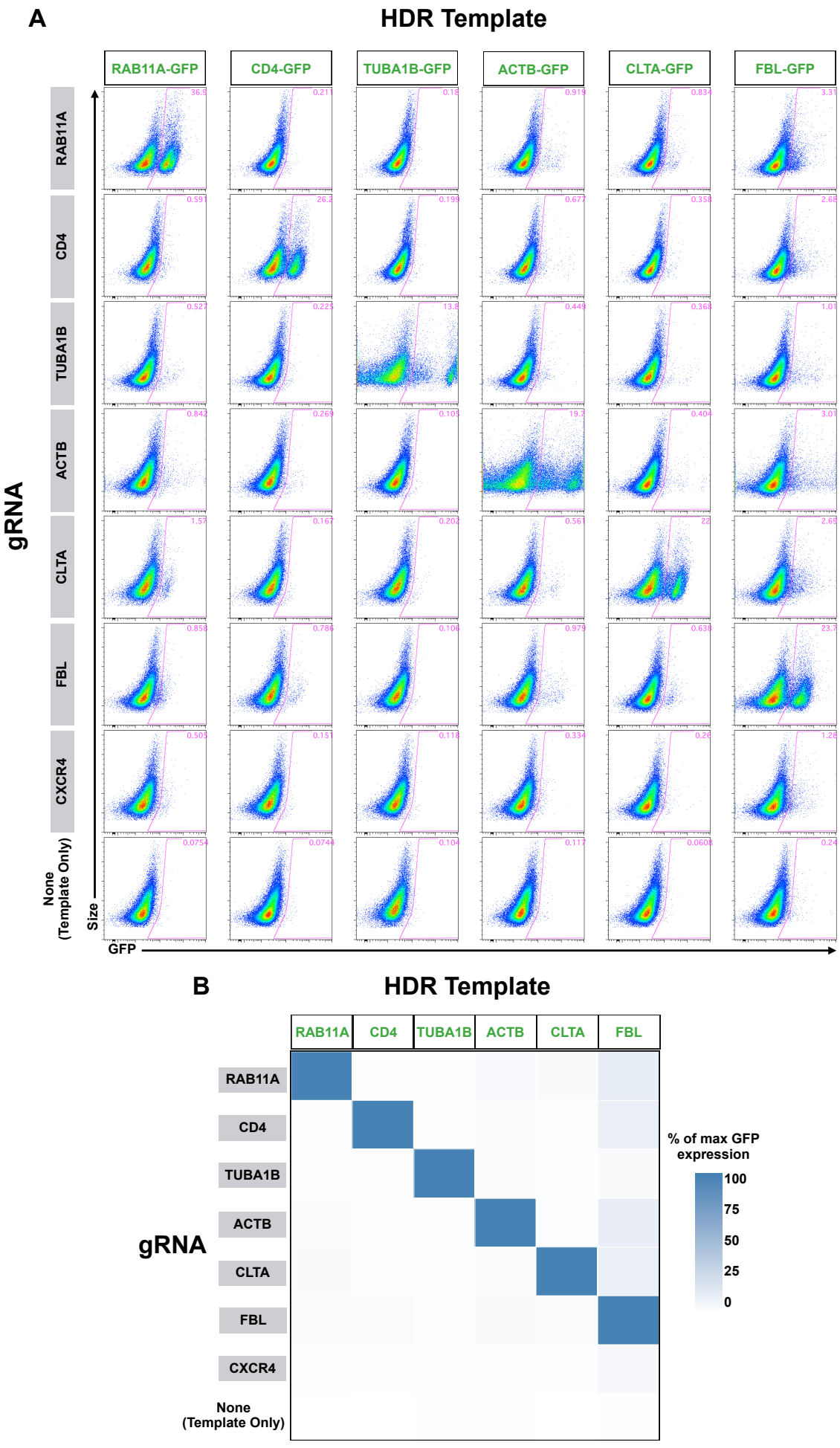
A
HDR Template
RAB11A-GFP
CD4-GFP
TUBA1B-GFP
ACTB-GFP
CLTA-GFP
FBL-GFP
gRNA
RAB11A
CD4
TUBA1B
ACTB
CLTA
FBL
CXCR4
None
(Template Only)
Size
GFP
B
HDR Template
RAB11A
CD4
TUBA1B
ACTB
CLTA
FBL
gRNA
CXCR4
None
(Template Only)
% of max GFP
expression
100
75
50
25
0

Sup Fig 14

Fig. S14. GFP expression across a HDR template versus gRNA matrix
(A) GFP expression was analyzed in CD3+CD4+ primary human T cells from a healthy donor 7 days following electroporation of a matrix of dsDNA HDR templates and their corresponding gRNAs, along with a CXCR4 gRNA and a no RNP control. As expected with a dsDNA template, off-target integrations were seen across combinations, but for all gRNAs and HDR templates the highest GFP expression was seen in the on-target condition. **(B)** Heat map summary of flow cytometry data in (A). One HDR template, a C-terminal GFP fusion tag into the nuclear factor FBL, had consistently higher off-target expression across gRNAs.

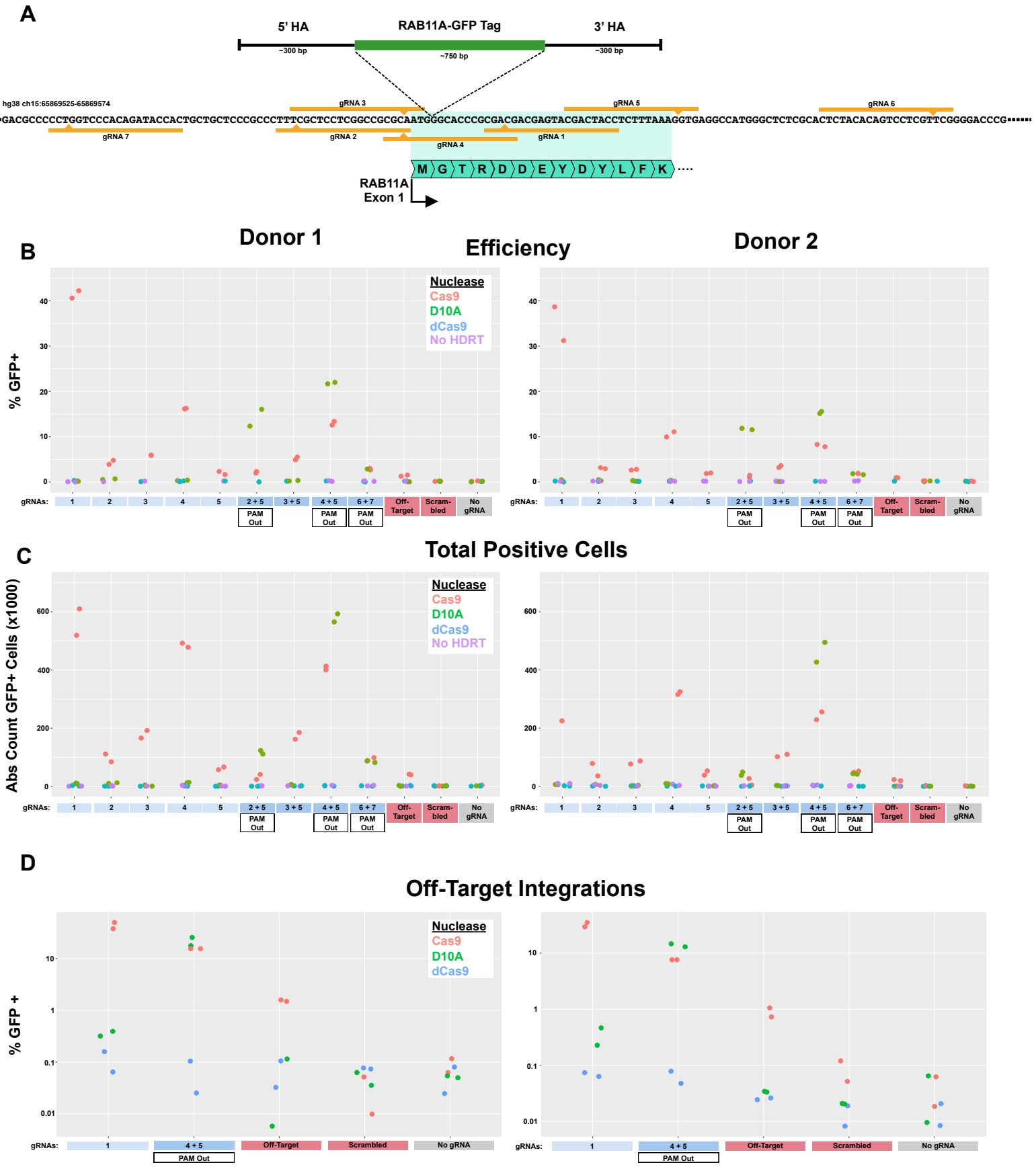
A
5' HA
RAB11A-GFP Tag
3' HA
~300 bp
~750 bp
~300 bp
hg38 ch15:65869525-65869574
GACGCCCCCTGGTCCCACAGATACCACTGCTGCTCCCGCCCTTTCGCTCCTCGGCCGCGCAATGGGCACCCGCGACGACGAGTACGACTACCTCTTTAAAGGTGAGGCCATGGGCTCTCGCACTCTACACAGTCCTCGTTCGGGGACCCG
gRNA 3
gRNA 5
gRNA 6
gRNA 7
gRNA 2
gRNA 4
gRNA 1
M G T R D D E Y D Y L F K
RAB11A
Exon 1
B
Donor 1
Efficiency
Donor 2
% GFP+
Nuclease
Cas9
D10A
dCas9
No HDRT
gRNAs:
1
2
3
4
5
2 + 5
3 + 5
4 + 5
6 + 7
Off-Target
Scram-bled
No gRNA
PAM Out
C
Total Positive Cells
Abs Count GFP+ Cells (x1000)
D
Off-Target Integrations
% GFP +
Scrambled

Sup Fig 15

Fig. S15. Efficient HDR in primary human T cells using a Cas9 nickase
(A) Diagram of the genomic locus containing the first exon of *RAB11A*. Use of spCas9 with a single guide RNA (gRNA 1) along with a dsDNA HDR template integrating a GFP in frame with RAB11A directly after the start codon results in efficient GFP expression (Fig 1F). Use of a Cas9 nickase (D10A variant) with two gRNAs could reduce the chances of off-target cutting. **(B-C)** A series of single gRNAs as well as dual gRNA combinations were tested for GFP insertion efficiency at the RAB11A N-terminal locus. As expected, no gRNAs showed appreciable levels of GFP insertion when using a nuclease dead Cas9 (dCas9). Multiple single gRNAs cutting adjacent to the insertion site showed GFP integration when using Cas9, but none as efficiently as gRNA 1. The D10A nickase showed little to no GFP integration with single guides, but with multiple two-guide combinations showed efficient GFP integration. Only in gRNA combinations where the two PAM sequences were directed away from each other (PAM Out) was GFP integration seen. **(D)** Raw data presented in (Fig 4C) demonstrating lower levels of functional off-target integrations when electroporating an off-target gRNA (targeting CXCR4), likely due to the requirement for the D10A nickase to have two gRNAs binding in close proximity to induce a dsDNA break. Dots in all displays (B-D) represent technical replicates in the labeled two healthy donors.

A

Exonuclease ssDNA production

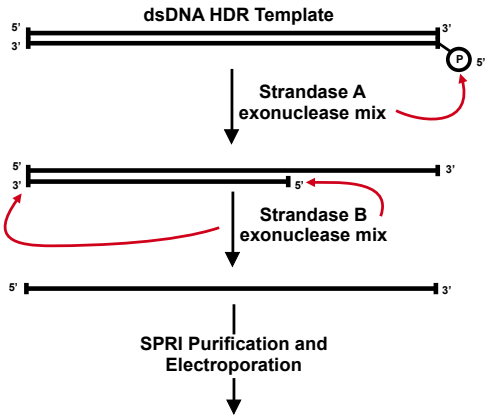

B

IVT-RT ssDNA production

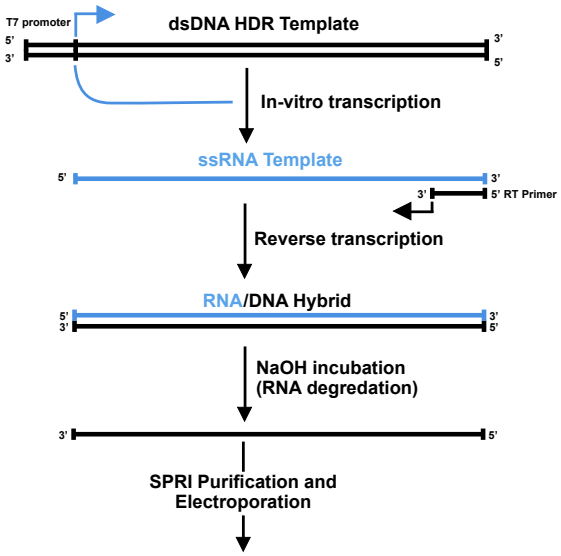

C

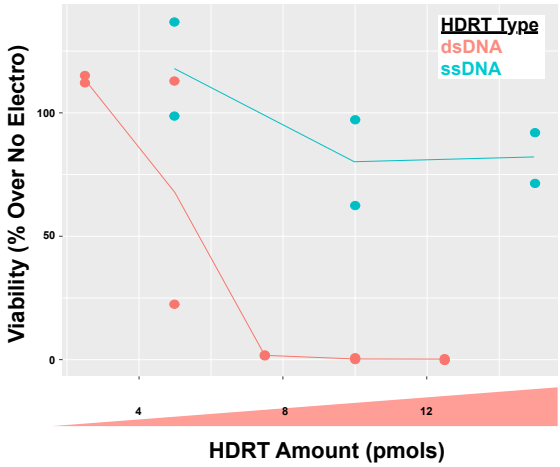

D

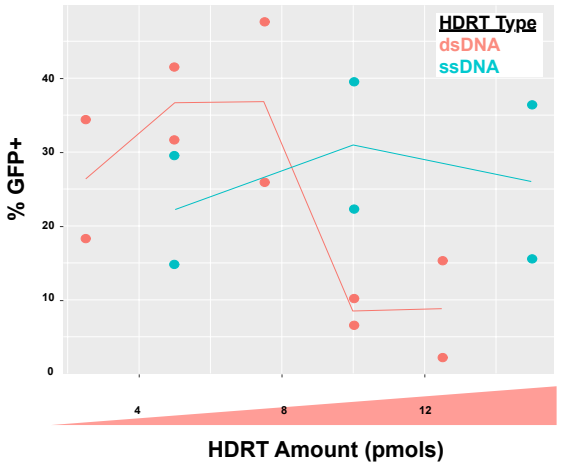

Sup Fig 16

Fig. S16. Multiple methods to produce long ssDNA HDR templates
(A) If a large enough amount of long single stranded DNA sequence could be produced for electroporation, off-target integrations could be reduced without overly compromising on-target efficiency. One method we developed involves a two step selective exonuclease digestion that specifically degrades one strand of a PCR product that has been labeled by 5' phosphorylation, easily added onto a PCR primer prior to amplification. **(B)** We also applied a second ssDNA production method based on sequential in-vitro transcription (IVT) and reverse transcription (RT) reaction. A PCR product with a short T7 promoter appended serves as an IVT template to produce a ssRNA product. Following annealing of an RT primer and reverse transcription, an RNA/DNA hybrid is formed which can be easily transformed into a long ssDNA template by incubation in sodium hydroxide (selectively degrades RNA strand). **(C)** At 2 days post-electroporation, viability in CD3+ T cells electroporated with only a ssDNA template was higher than those electroporated with only a dsDNA template (fig. S1). **(D)** A ssDNA RAB11A-GFP HDR template showed high efficiency GFP integration similar to dsDNA templates, and maintained high efficiency integrations at higher molar amounts of template, potentially due to increased viability (C) as well as less mass per mole of DNA template. Individual points represent at least two healthy donors (C, D)

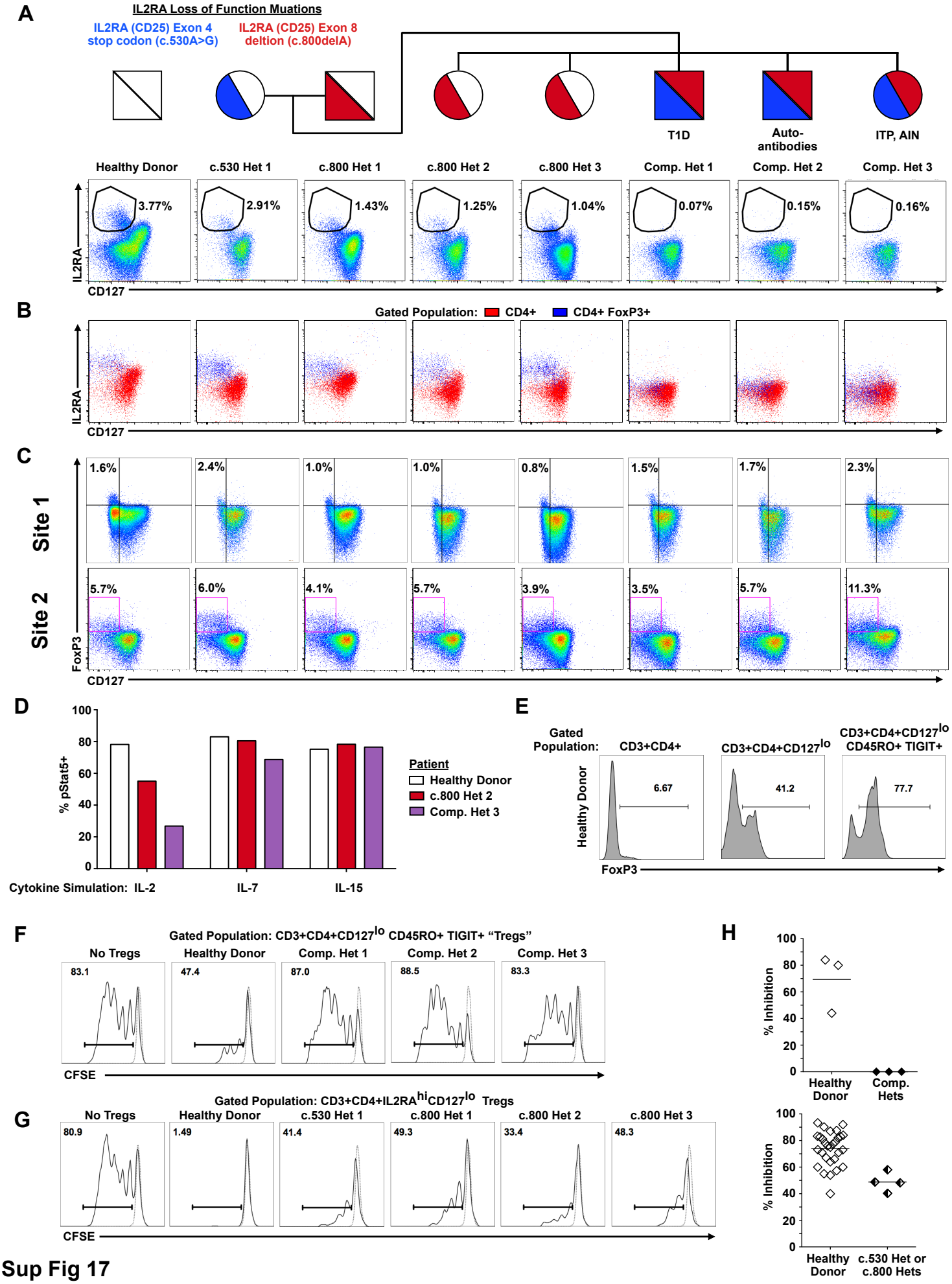
A
IL2RA Loss of Function Muations
IL2RA (CD25) Exon 4 stop codon (c.530A>G)
IL2RA (CD25) Exon 8 deltion (c.800delA)
T1D
Auto-antibodies
ITP, AIN
Healthy Donor
c.530 Het 1
c.800 Het 1
c.800 Het 2
c.800 Het 3
Comp. Het 1
Comp. Het 2
Comp. Het 3
3.77%
2.91%
1.43%
1.25%
1.04%
0.07%
0.15%
0.16%
IL2RA
CD127
B
Gated Population: CD4+ CD4+ FoxP3+
C
Site 1
Site 2
1.6%
2.4%
1.0%
1.0%
0.8%
1.5%
1.7%
2.3%
5.7%
6.0%
4.1%
5.7%
3.9%
3.5%
5.7%
11.3%
FoxP3
D
% pStat5+
Patient
Healthy Donor
c.800 Het 2
Comp. Het 3
Cytokine Simulation: IL-2 IL-7 IL-15
E
Gated Population:
CD3+CD4+
CD3+CD4+CD127lo
CD3+CD4+CD127lo CD45RO+ TIGIT+
Healthy Donor
6.67
41.2
77.7
FoxP3
F
Gated Population: CD3+CD4+CD127lo CD45RO+ TIGIT+ "Tregs"
No Tregs
Healthy Donor
Comp. Het 1
Comp. Het 2
Comp. Het 3
83.1
47.4
87.0
88.5
83.3
CFSE
G
Gated Population: CD3+CD4+IL2RAhiCD127lo Tregs
No Tregs
Healthy Donor
c.530 Het 1
c.800 Het 1
c.800 Het 2
c.800 Het 3
80.9
1.49
41.4
49.3
33.4
48.3
CFSE
H
% Inhibition
Healthy Donor
Comp. Hets
% Inhibition
Healthy Donor
c.530 Het or c.800 Hets

Sup Fig 17

Fig. S17. Reduced Treg frequencies and defective Treg suppressive capacity in subjects with two loss of function IL2RA mutations.
(A) CD3+CD4+ T cells from a healthy donor and all family members, including *IL2RA* heterozygotes (c.530 het 1, c.800 hets 1-3) as well as compound heterozygote children (Comp. Hets 1-3), with loss-of-function *IL2RA* mutations were analyzed by flow cytometry to assess presence of CD25hiCD127lo Tregs. **(B)** In healthy donors and single hets, CD4+FoxP3+ T cells are predominantly CD25hiCD127lo. In the compound heterozygotes, a CD127lo CD4+FoxP3+ population is present, but does not express IL2RA. **(C)** Clinical phenotyping performed at two separate sites confirms compound heterozygotes possess normal frequencies of CD127lo FoxP3+ cells. **(D)** Deficiency in IL2RA surface expression in compound heterozygote 3 led to aberrant downstream signalling as measured by pStat5 expression after stimulation with IL-2, but not IL-7 or IL-15. **(E)** Due to the inability to sort CD25hi Tregs from the CD25-deficient compound heterozygotes, an alternate gating strategy was established to enrich for FoxP3+ cells from CD3+CD4+ T cells using the surface markers CD127loCD45RO+TIGIT+. Intracellular FoxP3 staining from the indicated gated population is shown. **(F)** While these CD3+CD4+CD127loCD45RO+TIGIT+ potential "Tregs" were highly enriched for FoxP3 and showed some suppressive capacity when cultured with CFSE-labeled stimulated responder T cells (Tresps) from healthy donors, CD3+CD4+CD127loCD45RO+TIGIT+ from the compound heterozygotes showed no suppressive ability. Stimulated Tresp population (Solid curves), non-stimulated Tresp (Dashed curve). **(G)** Correction of either CD25 mutation in the compound heterozygotes individually would still leave the other mutation, leaving the cells as single heterozygotes. To confirm that such a potential correction would result in some level of functional suppression, CD4+CD25hiCD127lo Tregs from the c.530 and c.800 single heterozygote family members were isolated and their suppressive ability was assayed as in (F). **(H)** Dot plot summaries of Treg suppressive ability in cells from healthy donor, CD25-deficient compound heterozygotes (F) and CD25+/- c.530 or c.800 heterozygotes (G). While CD3+CD4+CD127loCD45RO+TIGIT+ "Tregs" from compound heterozygotes showed no suppressive ability, conventional CD4+CD25hiCD127lo Tregs from the single heterozygote family members showed some suppressive capacity, consistent with their lack of pronounced clinical phenotype compared to the compound hets.

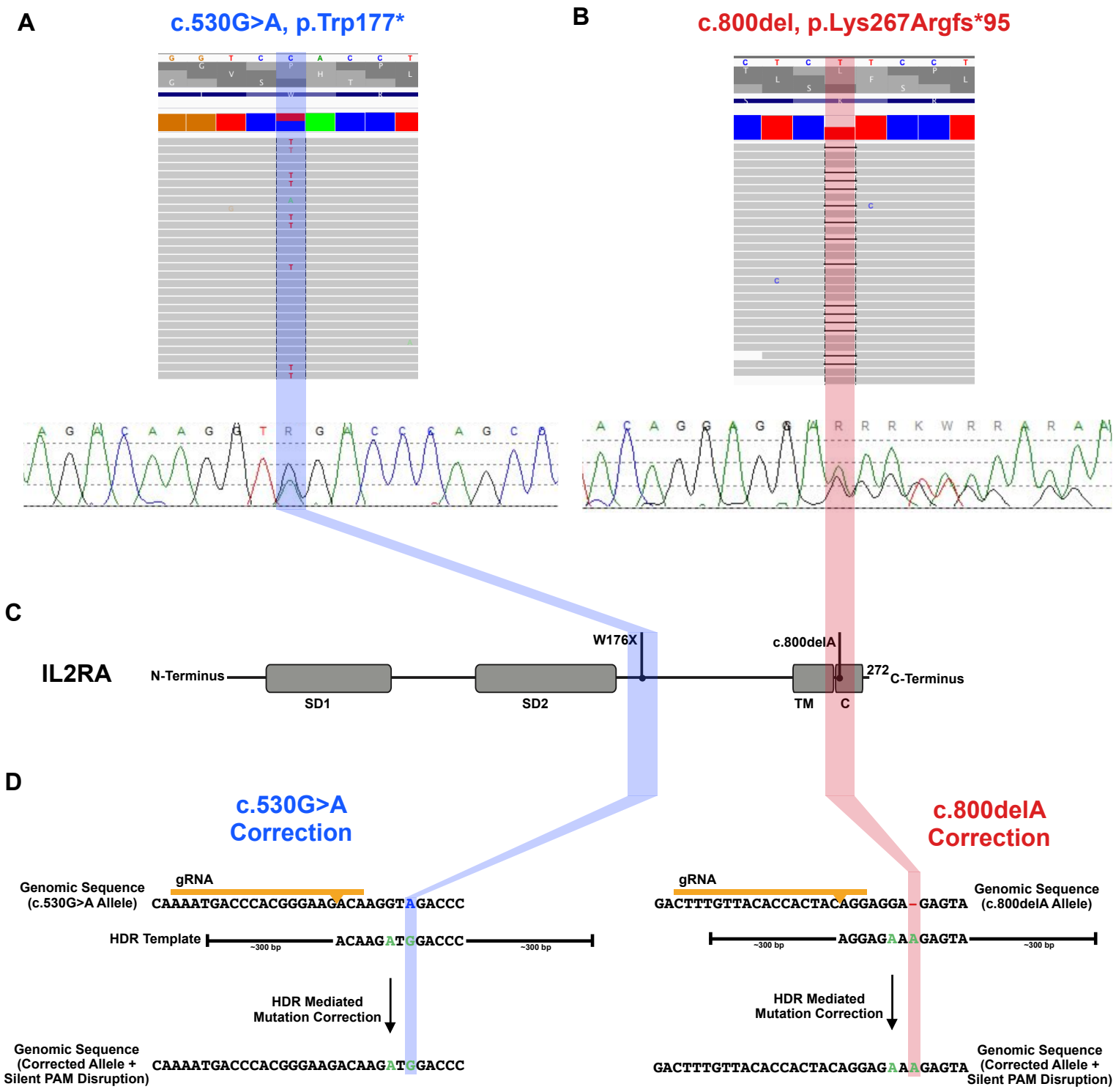
A
c.530G>A, p.Trp177*
B
c.800del, p.Lys267Argfs*95
C
IL2RA
N-Terminus
SD1
SD2
W176X
c.800delA
272
C-Terminus
TM
C
D
c.530G>A
Correction
Genomic Sequence
(c.530G>A Allele)
gRNA
CAAAATGACCCACGGGAAGACAAGGTAGACCC
HDR Template
~300 bp
ACAAGATGGACCC
~300 bp
HDR Mediated
Mutation Correction
Genomic Sequence
(Corrected Allele +
Silent PAM Disruption)
CAAAATGACCCACGGGAAGACAAGATGGACCC
c.800delA
Correction
gRNA
GACTTTGTTACACCACTACAGGAGGA–GAGTA
Genomic Sequence
(c.800delA Allele)
~300 bp
AGGAGAAAGAGTA
~300 bp
HDR Mediated
Mutation Correction
GACTTTGTTACACCACTACAGGAGAAAGAGTA
Genomic Sequence
(Corrected Allele +
Silent PAM Disruption)

Sup Fig 18

Fig. S18. Identification of compound heterozygous mutations in IL2RA and design of corrective CRISPR-Cas9 genome targeting reagents.
(A) Initial genetic testing of the proband (supplementary text) using an in-house targeted next-generation sequencing multi-gene panel of over 40 genes known to be involved in monogenic forms of diabetes was negative. Subsequent exome sequencing in the trio of proband and parents revealed two causative mutations in the *IL2RA* gene. The mother possessed a single heterozygous mutation (c.530G>A) in exon 4 of *IL2RA*, resulting in a premature stop codon. **(B)** The father possessed a single heterozygous mutation (c.800delA) in exon 8 of IL2RA, resulting in a frameshift mutation resulting in a 95 amino acid long run-on. Sanger sequencing confirmed that the proband was a compound heterozygote for both mutations. **(C)** A linear depiction of the IL2RA protein annotated with approximate locations of the two identified IL2RA mutations. SD1, sushi domain 1; SD2, sushi domain 2; TM, transmembrane; C, cytoplasmic. **(D)** The genomic sequences including the specified mutations were used to design CRISPR-Cas9 genome targeting reagents to correct the two *IL2RA* mutations. A gRNA was designed to cut adjacent to the site of each mutation, 8 bps away for c.530 mutation (Blue), and 7 bps away for c.800 (Red). For each mutation, an HDR template was designed including the corrected sequence (Green) as well as a silent mutation in a degenerate base to disrupt the PAM sequence ("NGG") for each guide RNA. Displayed genomic regions (not to scale) for c.530 mutation site (hg38 ch10:6021526-6021557) and c800 mutation site (hg38 ch10:6012886-6012917). Both ssODN HDR Templates (ssDNA with 60 bp homology arms), and large dsDNA or ssDNA HDR Templates (as displayed, with ~300 bp homology arms) were used (supplementary table 1).

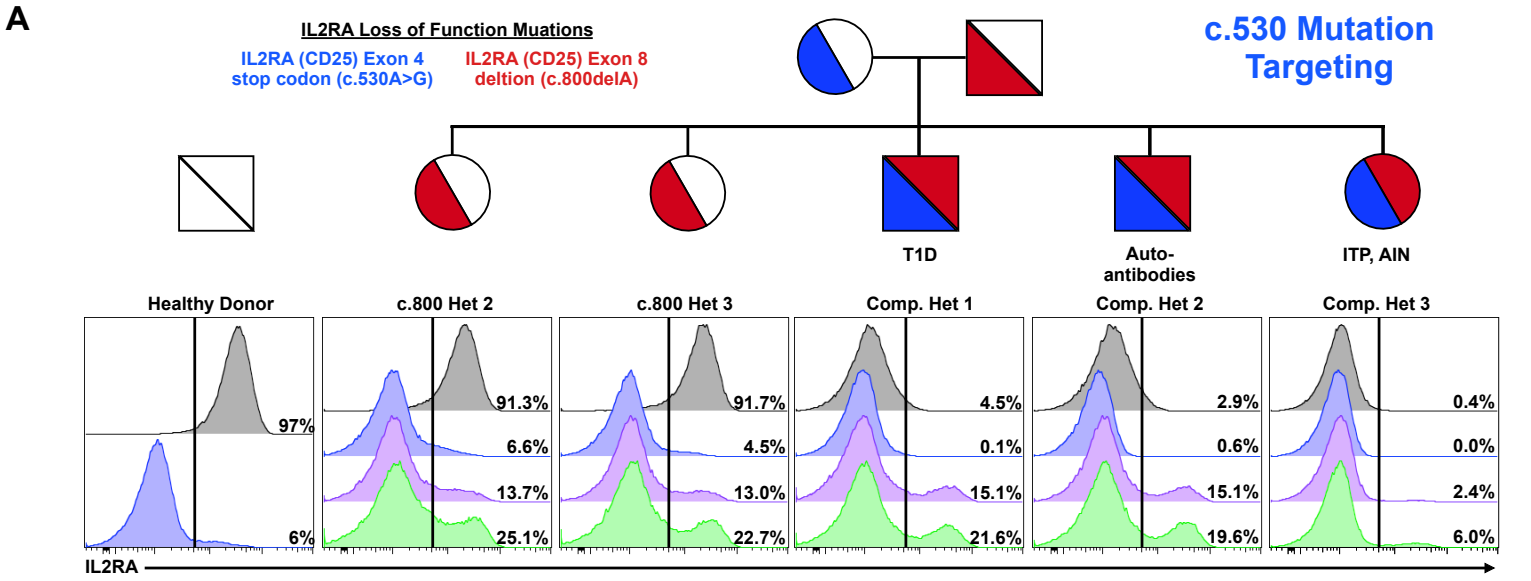
A
IL2RA Loss of Function Muations
IL2RA (CD25) Exon 4 stop codon (c.530A>G)
IL2RA (CD25) Exon 8 deltion (c.800delA)
c.530 Mutation Targeting
T1D
Auto-antibodies
ITP, AIN
Healthy Donor
c.800 Het 2
c.800 Het 3
Comp. Het 1
Comp. Het 2
Comp. Het 3
97%
6%
91.3%
6.6%
13.7%
25.1%
91.7%
4.5%
13.0%
22.7%
4.5%
0.1%
15.1%
21.6%
2.9%
0.6%
15.1%
19.6%
0.4%
0.0%
2.4%
6.0%
IL2RA

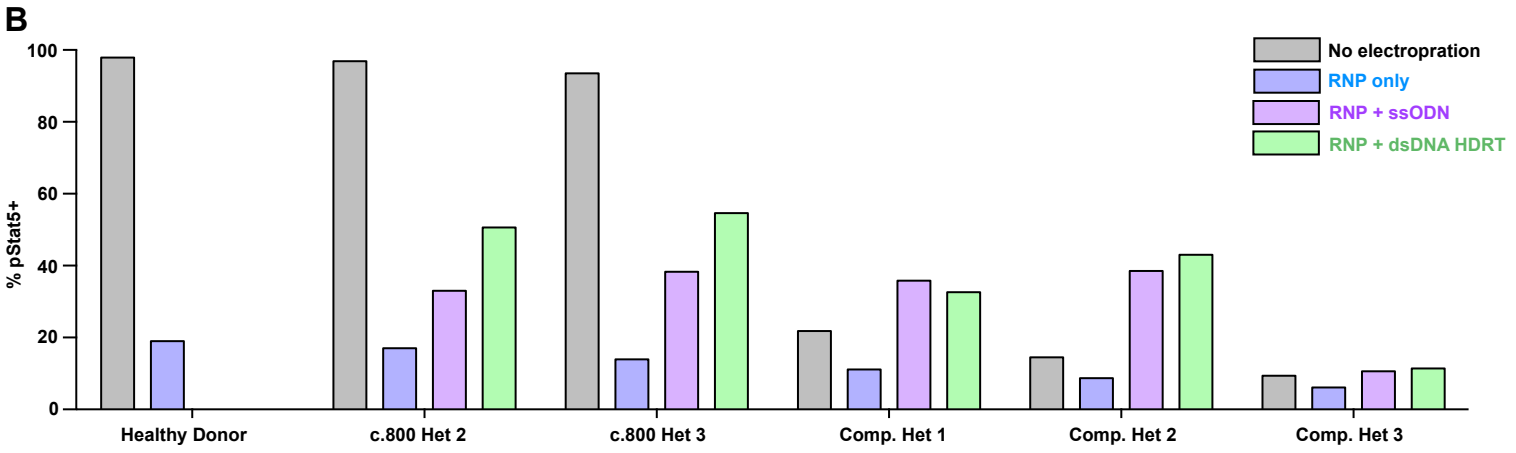
B
% pStat5+
100
80
60
40
20
0
No electropration
RNP only
RNP + ssODN
RNP + dsDNA HDRT
Healthy Donor
c.800 Het 2
c.800 Het 3
Comp. Het 1
Comp. Het 2
Comp. Het 3

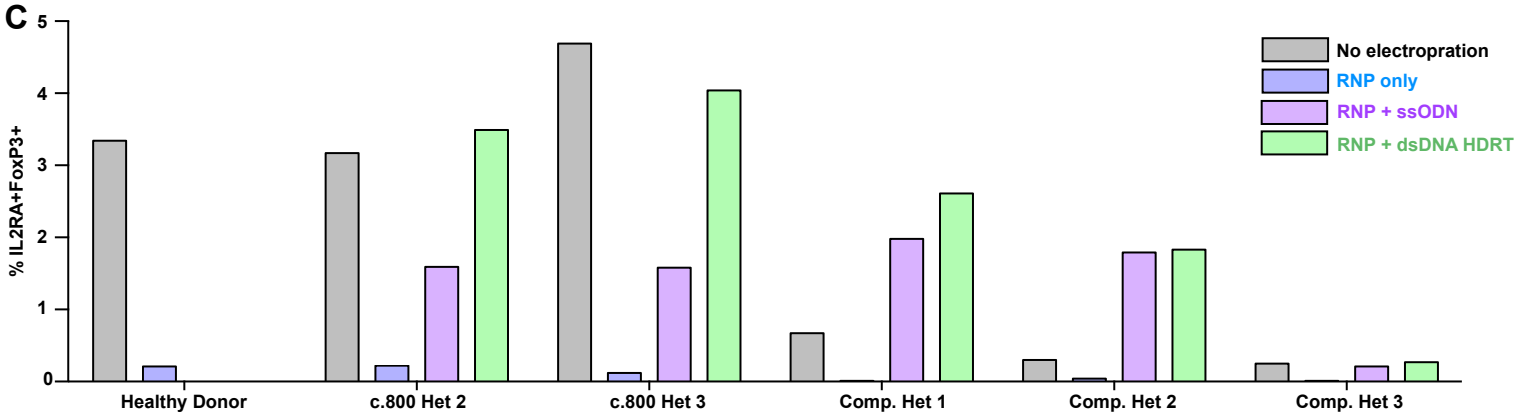
C
% IL2RA+FoxP3+
5
4
3
2
1
0
No electropration
RNP only
RNP + ssODN
RNP + dsDNA HDRT
Healthy Donor
c.800 Het 2
c.800 Het 3
Comp. Het 1
Comp. Het 2
Comp. Het 3

Sup Fig 19

Fig. S19. HDR mediated correction of IL2RA c.530A>G loss of function mutation
(A) Unlike the gRNA targeting the c.800delA mutation at the C-terminus of IL2RA (fig. S19), the gRNA targeting the c.530A>G mutation (causing a stop codon in an interior exon) results in substantial (~90%) knockdown of IL2RA in a healthy donor and single heterozygotes (c.800 Het 2 and 3) 2 days following electroporation of the RNP alone (Blue) into CD3+ T cells. While starting from a very small IL2RA+ percentage, knockdown was also observed in all three compound heterozygotes, potentially as some small amount of protein can be surface expressed off of the c.800delA allele. This reduced CD25 expression can be partially rescued by inclusion of an ssODN HDR template (Purple) and even more substantially rescued using a large dsDNA HDR template. Both template types contained the corrected sequence, a silent mutation to remove the gRNA's PAM sequence, and either 60 bp (ssODNs) or ~300 bp (large dsDNA) homology arms (Green) (fig. S18). Unlike targeting of the c.800delA mutation for correction, CD25 surface expression in T cells from the compound heterozygotes is only seen when an HDR template is included. In all three compound heterozygotes, the dsDNA HDR template yielded greater percentages of CD25+ cells. **(B)** Increased pStat5 signaling in response to IL-2 stimulation (200 U/mL) 7 days following electroporation in CD3+ T cells from compound heterozygote patients undergoing HDR-mediated mutation correction compared to no electroporation or RNP only controls. **(C)** Similarly, increased proportions of CD25+ FoxP3+ cells are seen 9 days following electroporation in the HDR correction conditions in compound heterozygote patients. Lower percentages of correction were seen when targeting the c.530 mutation for HDR correction in compound heterozygote 3, potentially due altered cell-state associated with the patient's disease or the patient's immunosuppressive drug regimen (fig. S23). Electroporations were performed according to optimized non-viral genome targeting protocol (Materials and Methods). For ssODN electroporations, 100 pmols in 1uL H2O were electroporated.

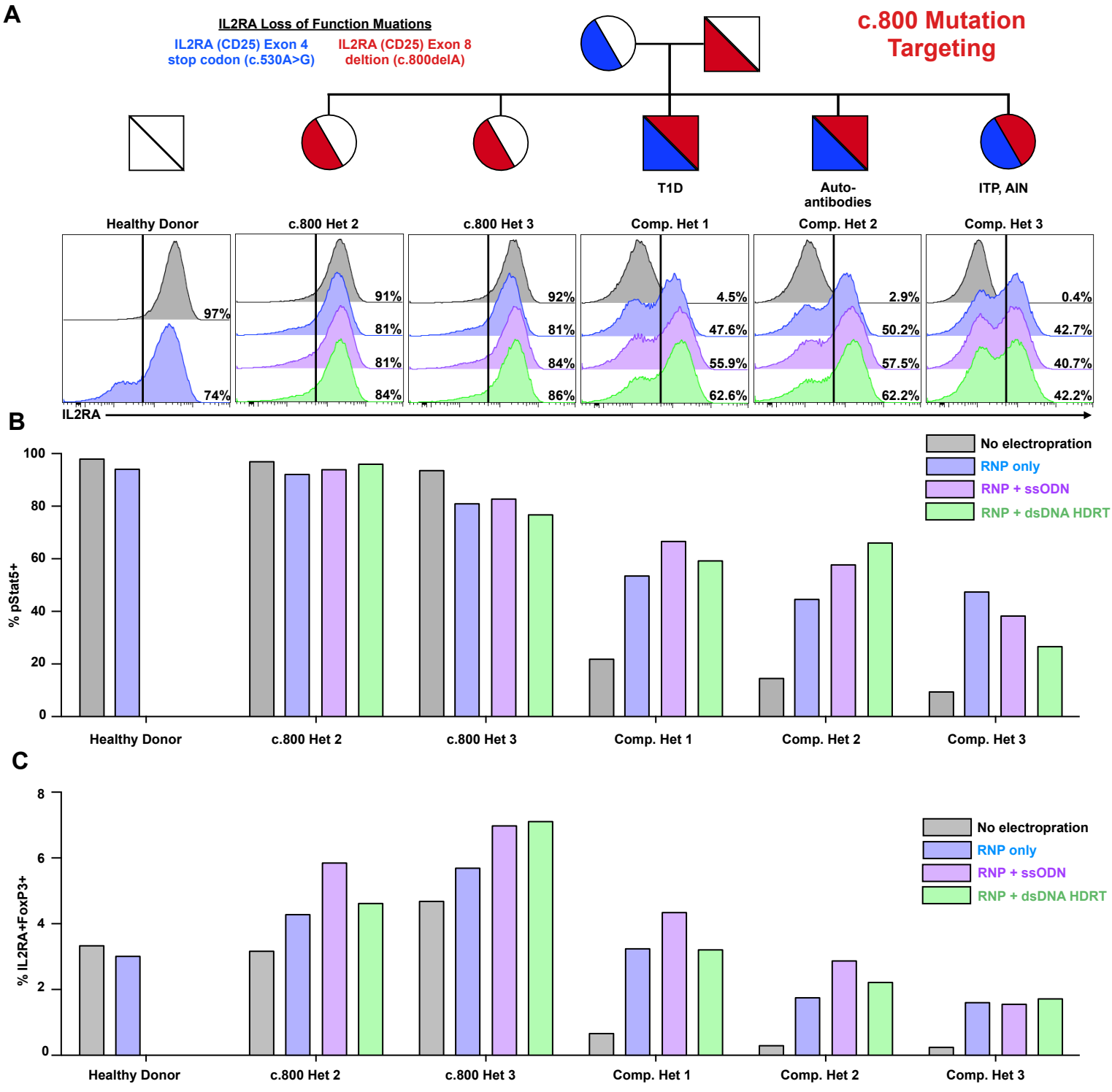
A
IL2RA Loss of Function Muations
IL2RA (CD25) Exon 4 stop codon (c.530A>G)
IL2RA (CD25) Exon 8 deltion (c.800delA)
c.800 Mutation Targeting
T1D
Auto-antibodies
ITP, AIN
Healthy Donor
c.800 Het 2
c.800 Het 3
Comp. Het 1
Comp. Het 2
Comp. Het 3
97%
74%
91%
81%
81%
84%
92%
81%
84%
86%
4.5%
47.6%
55.9%
62.6%
2.9%
50.2%
57.5%
62.2%
0.4%
42.7%
40.7%
42.2%
IL2RA
B
% pStat5+
No electropration
RNP only
RNP + ssODN
RNP + dsDNA HDRT
C
% IL2RA+FoxP3+

Sup Fig 20

Fig. S20. Non-HDR mediated correction of IL2RA c.800delA frameshift loss of function mutation

(A) Histograms of CD25 surface expression in CD3+ T cells in all children from a family carrying two loss-of-function *IL2RA* mutations, including three compound heterozygotes that express minimal amounts of IL2RA on their surface (No electroporation, Grey). Two days following electroporation of an RNP containing a gRNA against the site of one of the two mutations, a one base pair deletion in the final exon of *IL2RA* (c.800delA) causing a run-on past the normal stop codon, CD3+ T cells from a healthy donor and single hets (c.800 Het 2 and 3) show slight increase in CD25- cells (RNP only, Blue). Low knock-out is potentially due to the gRNA targeting the C-terminus of the protein where small indels may cause less pronounced loss of surface protein expression. Surprisingly, the RNP alone resulted in CD25 surface expression in almost 50% of edited T cells in all three compound heterozygotes. Increases in the percent of cells with CD25 correction compared to RNP only could be achieved by inclusion of an ssODN HDR template sequence with the mutation correction (RNP+ssODN, Purple), and further increased when using a longer dsDNA HDR template to correct the mutation (RNP + dsDNA HDRT, Green) (fig. S18). **(B)** Phospho Stat5 signaling in response to high dose IL-2 stimulation (200 U/mL) in edited CD3+ T cells following 7 days of expansion post-electroporation. Increased numbers of pStat5+ cells correlated with increases in CD25 surface expression (A). **(C)** Following 9 days of expansion post-electroporation, intracellular FoxP3 staining reveals a dramatically increased proportion of CD25+ FoxP3+ cells in CD3+ T cells compared to no electroporation controls, approaching the proportion of CD25+ FoxP3+ cells seen in a healthy donor similarly cultured. Electroporations were performed according to optimized non-viral genome targeting protocol (Materials and Methods). For ssODN electroporations, 100 pmols in 1uL H2O were electroporated.

A

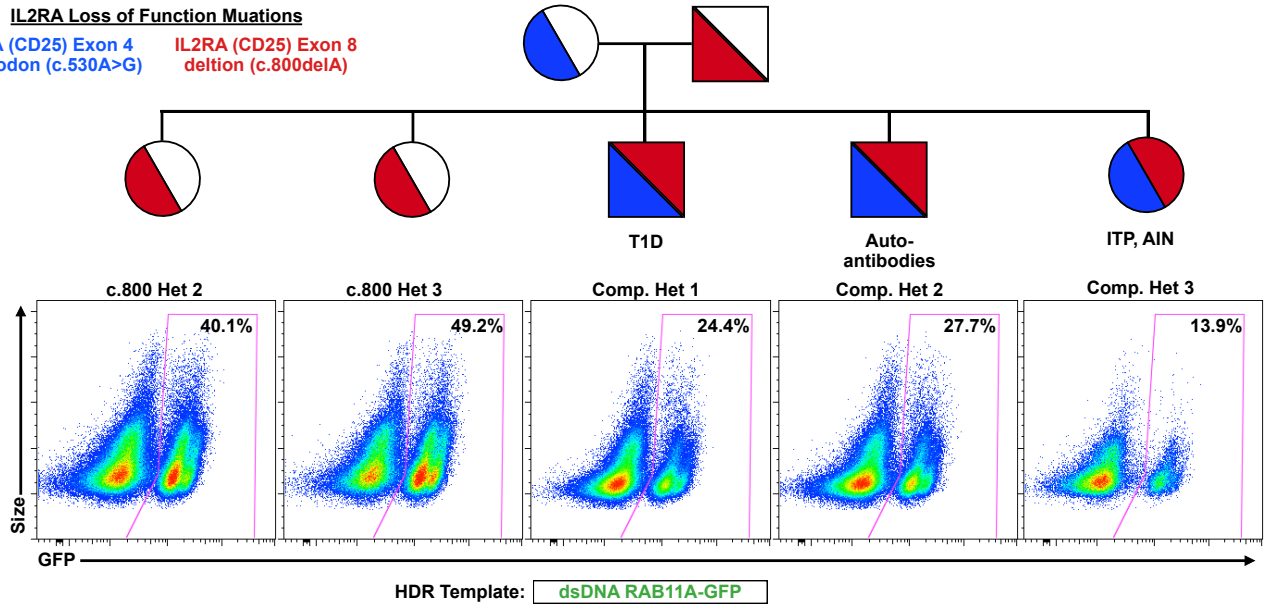
IL2RA Loss of Function Muations
IL2RA (CD25) Exon 4 stop codon (c.530A>G)
IL2RA (CD25) Exon 8 deltion (c.800delA)
T1D
Auto-antibodies
ITP, AIN
c.800 Het 2
c.800 Het 3
Comp. Het 1
Comp. Het 2
Comp. Het 3
40.1%
49.2%
24.4%
27.7%
13.9%
Size
GFP
HDR Template:
dsDNA RAB11A-GFP

B

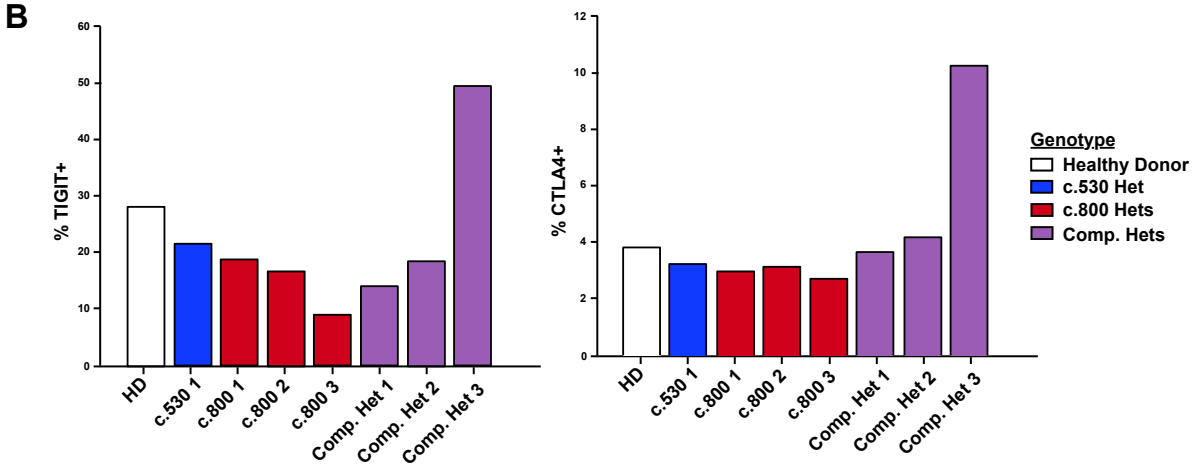
% TIGIT+
% CTLA4+
HD
c.530 1
c.800 1
c.800 2
c.800 3
Comp. Het 1
Comp. Het 2
Comp. Het 3
Genotype
Healthy Donor
c.530 Het
c.800 Hets
Comp. Hets

Sup Fig 21

Fig. S21. Diminished HDR potential and altered clinical phenotype in compound heterozygote IL2RA loss-of-function patient receiving immunosuppressants.
(A) Flow cytometric analysis of GFP expression 6 days following electroporation of a positive HDR control RAB11A-GFP dsDNA HDR template into CD3+ T cells from the indicated patients revealed lower GFP expression in the three compound heterozygotes compared to their two c.800 heterozygote siblings. Compared to a cohort of twelve healthy donors similarly edited (fig. S9), both c.800 heterozygotes as well as compound het 1 and 2 were within the general range observed across healthy donors, whereas compound het 3 had lower GFP expression than any healthy donor analyzed. Of note, while in compound het 3 HDR mediated correction at the c.530 mutation was substantially lower than the other two compound hets (Fig 5A), CD25 surface expression after electroporation of the c.800delA targeting RNP alone was similar. Unlike HDR mediated repair, a NHEJ mediated frameshift correction at c.800delA may not require cell proliferation, consistent with compound het 3 being the only compound heterozygote patient on active immunosuppressants at the time of blood draw and T cell isolation (supplementary text). **(B)** Altered cell-state associated with the patient's disease could also be contributory to diminished HDR rates. TIGIT and CTLA4 expression levels in non-edited, isolated CD4+ T cells from each indicated patient measured by flow cytometry. Consistent with altered activation state, cells from compound het 3 had a distinct phenotype, with increased TIGIT and CTLA4 expression compared both to healthy donors, the heterozygous family members, as well the other two compound heterozygous siblings.